http://doi.org/10.1093/plcell/koab292 THE PLANT CELL 2022: 34: 927–944

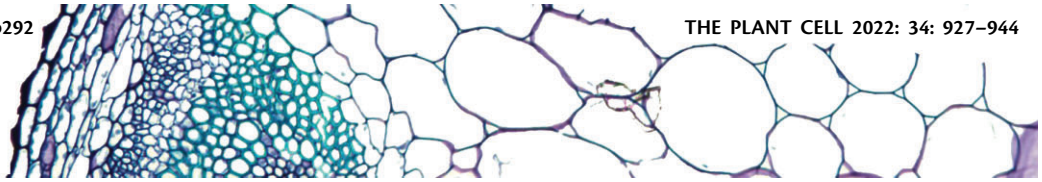

Research Article

PAMP-INDUCED SECRETED PEPTIDE 3 modulates salt tolerance through RECEPTOR-LIKE KINASE 7 in plants

Huapeng Zhou [1,*,†], Fei Xiao [1,2], Yuan Zheng [3], Guoyong Liu [4], Yufen Zhuang [1], Zhiyue Wang [1], Yiyi Zhang [1], Jiaxian He [1], Chunxiang Fu [5] and Honghui Lin [1,*,†]

1 Key Laboratory of Bio-resource and Eco-environment of Ministry of Education, College of Life Sciences, Sichuan University, Chengdu 610064, China
2 Xinjiang Key Laboratory of Biological Resources and Genetic Engineering, College of Life Science and Technology, Xinjiang University, Urumqi 830046, China
3 Department of Biology, Institute of Plant Stress Biology, State Key Laboratory of Cotton Biology, Henan University, Kaifeng 475004, China
4 State Key Laboratory of Plant Physiology and Biochemistry, College of Biological Sciences, China Agricultural University, Beijing 100193, China
5 Key Laboratory of Biofuels, Qingdao Institute of Bioenergy and Bioprocess Technology, Chinese Academy of Sciences, Qingdao 266101, China

*Author for correspondence: zhouhuapeng@scu.edu.cn (H.Z.) and hhlin@scu.edu.cn (H.L.)
†Senior authors
These authors contributed equally (H.Z., F.X., and Y.Z.).
H.Z. directed the project. H.Z. and F.X. designed the project, and F.X. performed the experiments with assistance of Y.Z., Y.F.Z., Z.W., and Y.Y.Z. G.L. contributed to analyze PIP3 subcellular localization. H.Z. and F.X. analyzed the data. H.Z., F.X., Y.Z., and C.F. contributed to discussion. H.Z. and F.X. wrote the manuscript. H.Z. and H.L. supervised the project.
The author responsible for distribution of materials integral to the findings presented in this article in accordance with the policy in the Instructions for Authors (https://academic.oup.com/plcell) is: Huapeng Zhou (zhouhuapeng@scu.edu.cn).

Abstract

High soil salinity negatively affects plant growth and development, leading to a severe decrease in crop production worldwide. Here, we report that a secreted peptide, PAMP-INDUCED SECRETED PEPTIDE 3 (PIP3), plays an essential role in plant salt tolerance through RECEPTOR-LIKE KINASE 7 (RLK7) in Arabidopsis (*Arabidopsis thaliana*). The gene encoding the PIP3 precursor, *prePIP3*, was significantly induced by salt stress. Plants overexpressing *prePIP3* exhibited enhanced salt tolerance, whereas a *prePIP3* knockout mutant had a salt-sensitive phenotype. PIP3 physically interacted with RLK7, a leucine-rich repeat RLK, and salt stress enhanced PIP3–RLK7 complex formation. Functional analyses revealed that PIP3-mediated salt tolerance is dependent on RLK7. Exogenous application of synthetic PIP3 peptide activated RLK7, and salt treatment significantly induced RLK7 phosphorylation in a PIP3-dependent manner. Notably, MITOGEN-ACTIVATED PROTEIN KINASE3 (MPK3) and MPK6 were downstream of the PIP3–RLK7 module in salt response signaling. Activation of MPK3/6 was attenuated in *pip3* or *rlk7* mutants under saline conditions. Therefore, MPK3/6 might amplify salt stress response signaling in plants for salt tolerance. Collectively, our work characterized a novel ligand–receptor signaling cascade that modulates plant salt tolerance in Arabidopsis. This study contributes to our understanding of how plants respond to salt stress.

Received October 25, 2021. Accepted November 25, 2021. Advance access publication December 3, 2021

Introduction

As a major abiotic stress, high soil salinity severely affects plant growth and crop productivity globally (Van Zelm et al., 2020). Climate change and inappropriate irrigation practices further exacerbate soil salinization, threatening worldwide food security (Cheeseman, 2016). Accumulated sodium ions (Na^+) in the soil reduce water availability for plants, leading to osmotic stress (Munns and Tester, 2008). Another detrimental effect caused by high NaCl concentrations is ionic toxicity for plants (Yang and Guo, 2018). The accumulation of Na^+ in the cytoplasm might replace essential potassium ions (K^+) and disrupt cellular ionic homeostasis, resulting in metabolic disorder in plant cells (Yang and Guo, 2018). Plants have evolved a variety of physiological and biochemical strategies to cope with elevated soil salinity to survive and complete their life cycles (Yang and Guo, 2018; Van Zelm et al., 2020). These adaptive responses are regulated by multiple signaling networks including ion exclusion and sequestration, metabolic refiguration, as well as growth and developmental adjustments (Zhu, 2016; Yang and Guo, 2018). For instance, the Salt Overly Sensitive (SOS) signaling pathway plays an essential role in maintaining ionic homeostasis in plants under saline conditions (Yang and Guo, 2018). Regulators of the SOS pathway such as 14-3-3 proteins and the GSK3-like kinase BRASSINOSTEROID (BR)-INSENSITIVE 2 have been functionally characterized and shown to fine-tune SOS-mediated ionic homeostasis and growth adjustment in plants responding to salt stress (Zhou et al., 2014; Li et al., 2020).

Peptide ligands have emerged as essential mediators of cell-to-cell communication during plant growth and stress responses (Matsubayashi and Sakagami, 2006; Matsubayashi, 2014). Based on their general features, more than 1,000 putative peptides have been identified in Arabidopsis (*Arabidopsis thaliana*) using bioinformatics tools (Lease and Walker, 2010). In general, peptides are characterized as small proteins with an N-terminal signal peptide (SP), a variable region in the middle, and a conserved C-terminus containing the active peptide (Matsubayashi, 2014). They are initially translated as propeptides and directed into the secretory pathway through their SP, and the propeptide can be proteolytically processed into an active peptide that may undergo additional specific modifications required for peptide–receptor binding (Matsubayashi, 2014; Chen et al., 2020). Through ligand–receptor interaction, peptide ligands might coordinate initial environmental stress responses to subsequent cellular signaling (Takahashi et al., 2019; Chen et al., 2020). For instance, CLAVATA 3/ENDOSPERM SURROUNDING REGION-RELATED 25 (CLE25) is an endogenous 12-amino acid (AA) peptide with two hydroxylated proline residues (Kondo et al., 2006). CLE25 effectively prevents water loss in Arabidopsis by transmitting a water deficit signal from the root to the shoot and controlling stomatal closure upon dehydration (Takahashi et al., 2018). In addition, an 11-AA peptide of CAP-DERIVED PEPTIDE 1 was reported to negatively regulate plant salt tolerance by downregulating the expression of salt tolerance genes under high salinity conditions (Chien et al., 2015). In contrast, the defense-related peptide PLANT ELICITOR PEPTIDE (Pep) AtPep3 derived from the AtPROPEP3 precursor peptide might prevent chlorophyll bleaching in plants grown under saline conditions (Nakaminami et al., 2018). Functional dissection revealed that AtPep3 can be recognized by its receptor PEP1 RECEPTOR 1 (PEPR1), whose loss of function nearly abolished AtPep3-induced salt resistance in Arabidopsis (Nakaminami et al., 2018). However, it should be noted that only a small fraction of predicted peptides has been currently functionally annotated or matched to a receptor.

Plant RECEPTOR-LIKE KINASEs (RLKs) belong to a large protein family with more than 600 members in Arabidopsis (Shiu et al., 2004), of which leucine-rich repeat (LRR)-RLKs (LRR-RLKs) represent the largest subfamily (Torii, 2004; Gou et al., 2010). A typical RLK contains an extracellular domain, a transmembrane domain, and a characteristic serine/threonine protein kinase domain (Torii, 2004). The extracellular domain may perceive a wide range of extracellular signals or ligands, leading to phosphorylation/activation of the intracellular kinase domain and subsequent activation of downstream signaling (Osakabe et al., 2013). Numerous studies have demonstrated that MITOGEN-ACTIVATED PROTEIN KINASE (MAPK) cascades might act downstream of RLKs in Arabidopsis (Meng et al., 2012; Li et al., 2014). In fact, MAPK cascades have been characterized as a hub of diverse signaling pathways (Asai et al., 2002; Mishra et al., 2006). RLKs are indeed involved in multiple signaling processes in plants, such as BR INSENSITIVE 1 for BR signaling (Li and Chory, 1997), FLAGELLIN-SENSITIVE 2 for plant immune responses (Gómez-Gómez and Boller, 2000), and HAESA for the regulation of abscission (Jinn et al., 2000). Importantly, RLKs also function in adaptive responses to salt stress. As mentioned above, the RLK PEPR1 is required for AtPep3-induced salt tolerance (Nakaminami et al., 2018). Another example is rice (*Oryza sativa*) SALT INTOLERANCE 1, a lectin-type RLK that modulates salt sensitivity by phosphorylating MPK3/MPK6, and mediates ethylene signaling as well as reactive oxygen species (ROS) homeostasis (Li et al., 2014). Furthermore, FERONIA (FER), a member from the *Catharanthus roseus* RLK1-like (*Cr*RLK1L) family in Arabidopsis, also regulates plant growth and salt tolerance (Zhao et al., 2018). FER, LEUCINE-RICH REPEAT EXTENSINs, and RAPID ALKALINIZATION FACTOR peptides may form a functional module that connects salt stress-induced cell-wall alterations to salt stress responses (Zhao et al., 2018). In addition, FER-dependent signaling may elicit a cell-specific calcium (Ca^{2+}) signal to maintain cell wall integrity during salt stress and root growth recovery after exposure to high salinity (Feng et al., 2018).

Despite the extensive knowledge provided by the previous studies, little is known regarding the functional role of peptide–RLK modules in plant salt tolerance signaling. Here, we show that Arabidopsis PAMP-INDUCED SECRETED PEPTIDE 3 (PIP3) modulates salt tolerance through RLK7. PIP3

physically interacts with RLK7 in planta, and salt stress enhances PIP3–RLK7 complex formation. PIP3-mediated salt tolerance requires RLK7, while salt treatment significantly induces RLK7 phosphorylation in a PIP3-dependent manner. MPK3 and MPK6 function downstream of PIP3–RLK7 module and possibly amplify salt stress signaling in plants, resulting in enhanced salt tolerance. Taken together, our work identified a ligand–receptor signaling cascade that modulates plant salt tolerance in Arabidopsis. The salt-activated PIP3–RLK7 module activates downstream MPK3/6 for plant resistance to salt stress. Our work enhances our understanding of plant salt tolerance, and provides putative targets for engineering salt-tolerant crops.

Results

Salt stress significantly upregulates *prePIP1* and *prePIP3* transcription

Arabidopsis PIP and PIP-LIKE (PIPL) peptides form a family consisting of 11 members (PIP1–3 and PIPL1–8) (Hou et al., 2014; Vie et al., 2015). Structurally, each of their precursors, prePIP/prePIPLs, possesses an N-terminal SP, a variable region in the middle, and one or two conserved core SGPS motif(s) in the C-terminus (Figure 1A). Phylogenic analysis using the full-length protein sequences of prePIP/prePIPLs revealed that they can be grouped into three clades, implying that there might exist functional divergence among PIP/PIPL members (Figure 1B). Previous studies showed that *prePIP/prePIPL* transcription is induced by a variety of biotic and/or abiotic stresses, with some *prePIP/prePIPL* genes specifically induced by salt stress (Vie et al., 2015), suggesting their possible regulatory role in plant salt stress response. As determined by real-time quantitative PCR (RT-qPCR) analysis of 10-day-old Columbia-0 (Col-0) seedlings left untreated or treated with 125-mM NaCl for the indicated time periods, we validated the transcriptional induction of *prePIP/prePIPL* genes by salt stress at different levels (Figure 1C). Among them, *prePIP1* and *prePIP3* were strongly upregulated upon salt exposure, and the induction of *prePIP3* expression was much higher than that of *prePIP1* (Figure 1C).

We generated a fusion construct consisting of the green fluorescent protein (GFP) coding sequence cloned in-frame and downstream of *prePIP3* or *prePIP1* and obtained the resulting independent transgenic plants *prePIP3pro:prePIP3-GFP* (*PIP3-OE*, *OE* designating [over]expression driven by the gene's promoter) and *prePIP1pro:prePIP1-GFP* (*PIP1-OE*) (Supplemental Figure S1, A, B, G and H). Immunoblot results showed that prePIP3 protein accumulates to a higher level more rapidly than prePIP1 when the transgenic plants were exposed to salt treatment for the indicated time periods (Figure 1, D and E), suggesting a possible role for PIP3 and PIP1 in plant salt responses.

To explore such a potential role, we generated transgenic plants overexpressing each *prePIP/prePIPL* except *prePIPL6* due to its low transcript abundance (Supplemental Figure S1, C–F). Phenotypic analyses demonstrated that, except for *35Spro:prePIP3-GFP* (*PIP3-OX*, *OX* designating overexpression driven by the 35S promoter) seedlings, all other transgenic lines display comparable salt sensitivity as the wild-type (WT) Col-0 (Supplemental Figure S2, A–C). In contrast, *PIP3-OX* seedlings exhibited higher germination and cotyledon greening rates than WT (Supplemental Figure S2, A–C). Together, these results demonstrated that PIP3 is possibly involved in plant salt tolerance regulation.

PIP3 modulates plant salt tolerance in Arabidopsis

PIP/PIPL peptides are predicted to be secreted to the apoplastic space (Matsubayashi, 2011; Hou et al., 2014; Vie et al., 2015). In fact, PIP1 was previously validated as a secreted peptide (Hou et al., 2014). To experimentally determine whether PIP3 is also secreted, we transiently co-infiltrated *prePIP3-GFP* and *PLASMA MEMBRANE (PM) INTRINSIC PROTEIN 2;1* (*PIP2;1*)*-mCherry* (Ma et al., 2015) constructs in *Nicotiana benthamiana* leaves. Following mannitol treatment, the plasmolyzed cells were observed by confocal microscopy. Similar to PIP1 (Hou et al., 2014), our plasmolysis assay revealed that PIP3-GFP fluorescence is indeed distributed in the apoplastic space (Figure 2A), indicating that PIP3 is a secreted peptide. In the plasmolysis assay, the PIP2;1-mCherry fusion protein was used as a PM marker (Figure 2A).

To further determine the regulatory role of PIP3 in plant salt tolerance, we carried out salt sensitivity assays using seedlings of Col-0 and *PIP3-OX* (lines #3, #4, and #6). When 4-day-old seedlings were transferred from Murashige and Skoog (MS) medium to fresh MS medium containing 125-mM NaCl, *PIP3-OX* seedlings displayed less growth inhibition for both root and shoot compared to Col-0 (Figure 2, B–D). In contrast, we observed no obvious growth difference between WT and *PIP3-OX* seedlings under control conditions of MS medium alone (Figure 2, B–D). As salt stress disrupts cellular ionic homeostasis in plants (Yang and Guo, 2018), we determined the intracellular Na^+ accumulation in root tips by staining with the fluorescent Na^+ indicator CoroNa Green (Oh et al., 2010). Root tip cells of *PIP3-OX* seedlings accumulated less Na^+ compared to WT seedlings when treated with salt (Figure 2, E and F). We also determined the Na^+ and K^+ contents in Col-0 and *PIP3-OX* seedlings: 2-week-old Col-0 and *PIP3-OX* seedlings grown on soil were left untreated or treated with 300-mM NaCl, and then subjected to atomic absorption spectrophotometer (AAS) analysis using shoot and root tissues separately. *PIP3-OX* seedlings accumulated less Na^+ but more K^+ than WT seedlings (Figure 2, G–J), leading to a lower Na^+/K^+ ratio in both shoots and roots (Supplemental Figure S3, A and B). In addition, soil-grown *PIP3-OX* plants exhibited better growth with higher chlorophyll contents than Col-0 exposed to the same salt treatment (Supplemental Figure S4, A–C). In all experiments, we observed no differences for plant growth or ion contents among the tested genotypes grown under normal growth conditions (Figure 2, E–J; Supplemental Figure S4).

We also generated *pip3* homozygous mutants (lines #1 and #2) that harbor a 47-bp deletion in *prePIP3* using clustered

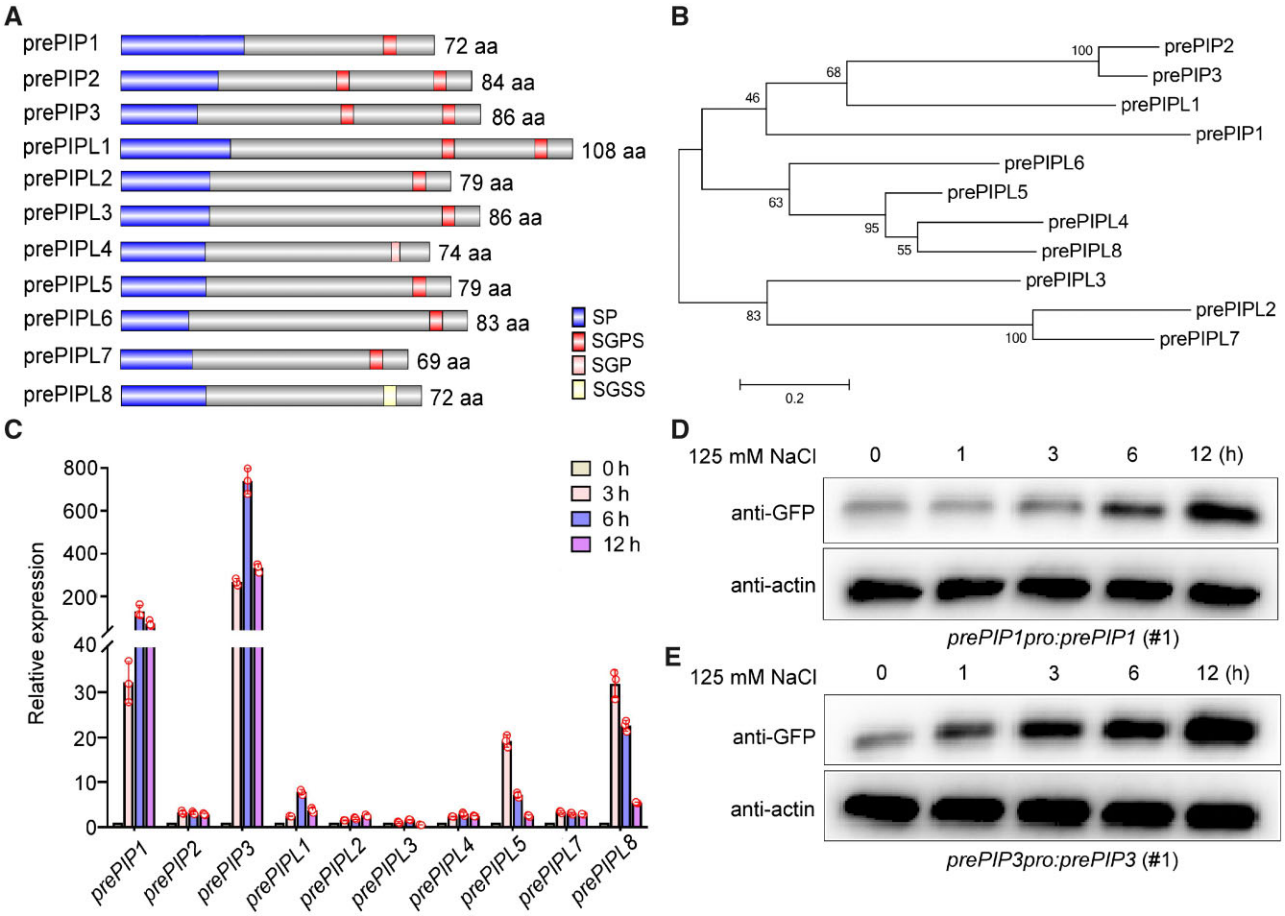

Figure 1 *prePIP1* and *prePIP3* are highly induced by salt stress. A, Schematic representation of prePIP/prePIPLs. Blue boxes represent the SP identified by SignalP version 4.1, while gray boxes indicate variable regions, and various shades of red boxes represent the conserved domains (SGPS, SGP, and SGSS) among PIP/PIPL peptides. B, Phylogenetic analysis of prePIP/prePIPL family members. The phylogenetic tree was constructed based on the protein sequence alignment of prePIP/prePIPLs using the neighbor-joining method with 1,000 bootstrap replicates in MEGA6. The values at the nodes represent percent of bootstrap confidence level. The scale bar 0.2 indicates AA substitutions per site. C, RT-qPCR analysis of *PIP/PIPL* transcript levels in 10-day-old Col-0 seedlings left untreated or treated with 125-mM NaCl for the indicated times. *ACTIN 2* was used as the internal control. Expression levels in Col-0 under control conditions were set to 1. Error bars represent SD ($n = 3$). Results are shown from one representative out of three independent experiments. D and E, Immunoblot assays for prePIP1 and prePIP3 abundance. Ten-day-old *prePIP1pro:prePIP1-GFP* (D) and *prePIP3pro:prePIP3-GFP* (E) seedlings were left untreated or treated with 125-mM NaCl for the indicated times. Then total proteins were extracted and detected with anti-GFP and anti-actin antibodies.

regularly interspaced short palindromic repeats (CRISPR)/Cas9-mediated gene editing (Supplemental Figure S5, A and B). Salt sensitivity analysis showed that *pip3* seedlings display slower growth compared to Col-0 under saline conditions (Figure 3, A–C). We also observed that *pip3* seedlings have lower germination and cotyledon greening rates than Col-0 when treated with salt (Supplemental Figure S5, C–E). In agreement, CoroNa Green staining revealed more Na^+ accumulating in the root tip cells of *pip3* seedlings relative to Col-0 (Figure 3, D and E). To determine whether the salt-sensitive phenotype seen in *pip3* was due to the loss of PIP3, we constructed the complementation lines *pip3 prePIP3pro:prePIP3-GFP* (*PIP3-COM*, lines #1 and #2; Supplemental Figure S1A). Phenotypic analysis revealed that the transgenic genomic copy of *prePIP3* fully rescues the salt sensitivity of *pip3* back to WT levels (Supplemental Figure S5, F–H).

We next performed exogenous applications of synthetic PIP3 peptide. Accordingly, a peptide was synthesized comprising the last 35 AAs of the prePIP3 C-terminus including two conserved SGPS motifs. Using a liquid culture-based salt sensitivity assay with 7-day-old Col-0 and *pip3* (line #1) seedlings, *pip3* mutant seedlings exhibited a stronger retarded growth with lower fresh weight and chlorophyll contents compared to Col-0 under saline conditions (Figure 3, F–H). Notably, the salt-sensitive phenotype of *pip3* seedlings was nearly rescued to Col-0 levels when synthetic PIP3 peptide was added to the medium (Figure 3, F–H). Taken together, these results demonstrated that the reduced plant salt tolerance of *pip3* plants is due to the loss of PIP3 function. We also performed phenotypic assays using Col-0 and *PIP1-OX* seedlings, which displayed comparable salt sensitivity (Supplemental Figure S6, A–C). Exogenous application of

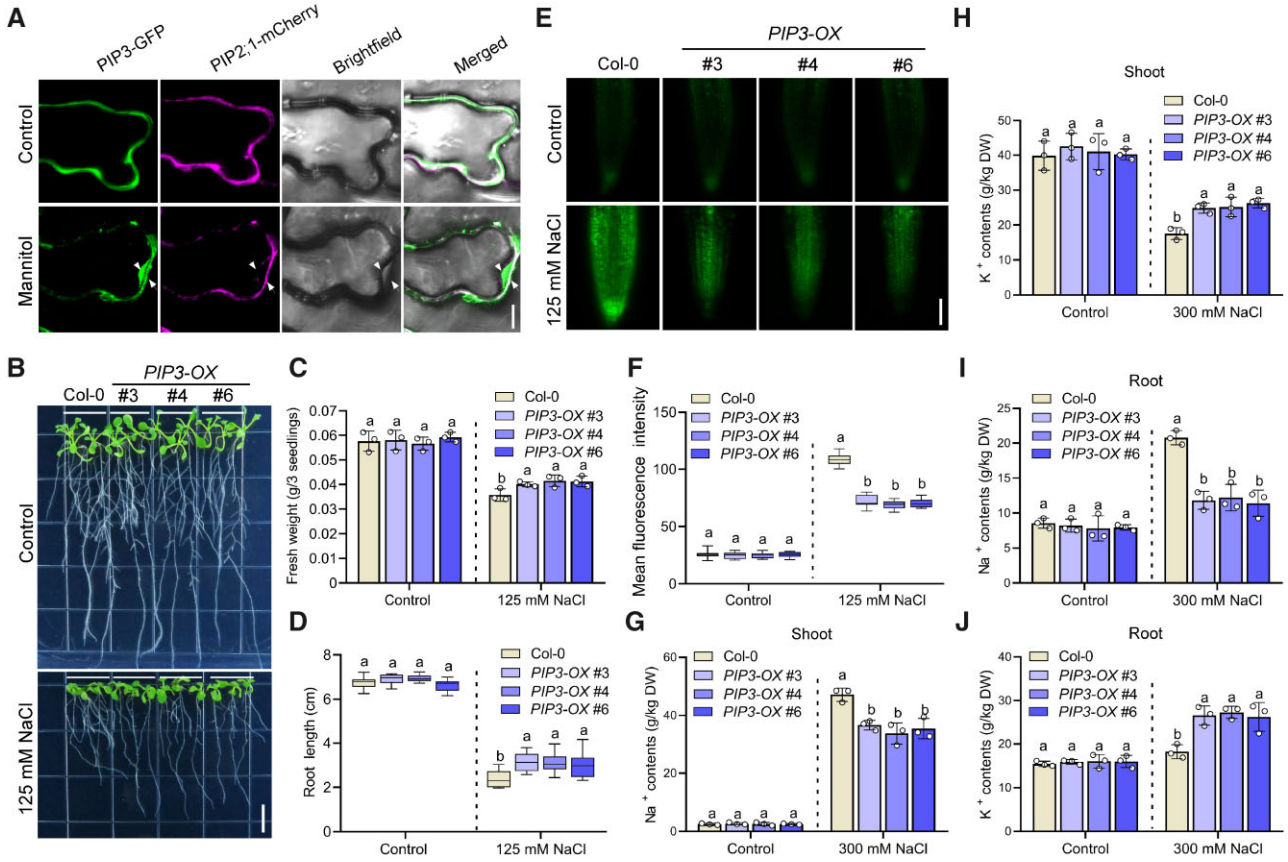

Figure 2 Overexpression of *prePIP3* enhances plant salt tolerance. A, Subcellular localization analysis of PIP3. The *35Spro:prePIP3-GFP* construct was transiently infiltrated in *N. benthamiana* leaves with *PIP2;1-mCherry* construct as PM marker. After additional growth for 2 days, infiltrated *N. benthamiana* leaves were left untreated or treated with 1-M mannitol for 30 min, then the fluorescence of GFP or mCherry was detected by a Leica SP5 microscope. White arrowhead indicates apoplastic space. Bar = 10 μm. B, Salt sensitivity analysis. Four-day-old Col-0 and *35Spro:prePIP3-GFP* (*PIP3-OX*) seedlings were transferred to MS medium or MS medium containing 125-mM NaCl for additional growth, and the photographs were taken 7 day after transfer. Bar = 1 cm. C and D, Quantification of fresh weight (C) and root length (D) of plants in (B). Data are presented as means ± SD (n = 3 for [C] or n = 9 for [D]). Results are shown from three independent experiments. Different lowercase letters indicate a significant difference at $P < 0.05$ based on one-way analysis of variance (ANOVA). E, CoroNa Green staining. Seedlings of 4-day-old Col-0 and *PIP3-OX* left untreated or treated with 125-mM NaCl for 12 h were stained with CoroNa Green. Representative root tips are shown. Bar = 100 μm. F, Mean CoroNa Green fluorescence intensity in (E). Data are presented as means ± SD (n = 9). Results are shown from three independent experiments. Different lowercase letters indicate a significant difference at $P < 0.05$ based on ANOVA. G–J, Determination of Na^+ and K^+ contents in plants. Two-week-old Col-0 and *PIP3-OX* seedlings grown on soil were left untreated or treated with 300-mM NaCl for 7 days, and the shoots and roots were collected separately to measure Na^+ (G and I) and K^+ (H and J) contents using AAS. Data are presented as means ± SD (n = 3). Results are shown from three independent experiments. Different lowercase letters indicate a significant difference at $P < 0.05$ based on ANOVA.

synthetic PIP1 peptide also had no effect on plant salt tolerance in WT (Supplemental Figure S6, D–F). Taken together, these results suggested that PIP3 mediates plant salt tolerance, possibly through regulating cellular ionic homeostasis, while PIP1 might not be implicated in plant salt tolerance.

PIP3 physically interacts with RLK7

Most studied small secreted peptides were reported to be recognized by PM-localized LRR-RLKs (Murphy et al., 2012). To identify the possible PIP3 receptor, we generated the binary construct *35Spro:prePIP3-nYFP* to screen for PIP3-interacting protein(s) using bimolecular fluorescence complementation (BiFC) assays in *N. benthamiana* leaves. We detected the reconstitution of yellow fluorescent protein (YFP) fluorescence signals in leaves transiently co-infiltrated with *prePIP3-nYFP* and *RLK7-cYFP* constructs, but not in leaves expressing other construct combinations (Figure 4A). As a previous study reported an absence of interaction between RLK7 and BIK1 (Hou et al., 2014), we used the RLK7/BIK1 combination as a negative control. Interestingly, the LRR-RLK RLK7 was previously identified as a PIP1 receptor for plant defense signaling (Hou et al., 2014) and a PIPL3 receptor for lateral root development in Arabidopsis (Toyokura et al., 2019).

We conducted a semi in vivo pull-down assay to confirm that PIP3 physically interacts with RLK7. Accordingly, we incubated purified recombinant glutathione S-transferase (GST)-tagged prePIP3 protein with protein extracts from *35Spro:RLK7-Flag* transgenic seedlings (Supplemental Figure S7A). RLK7-Flag was clearly pulled down with prePIP3-GST

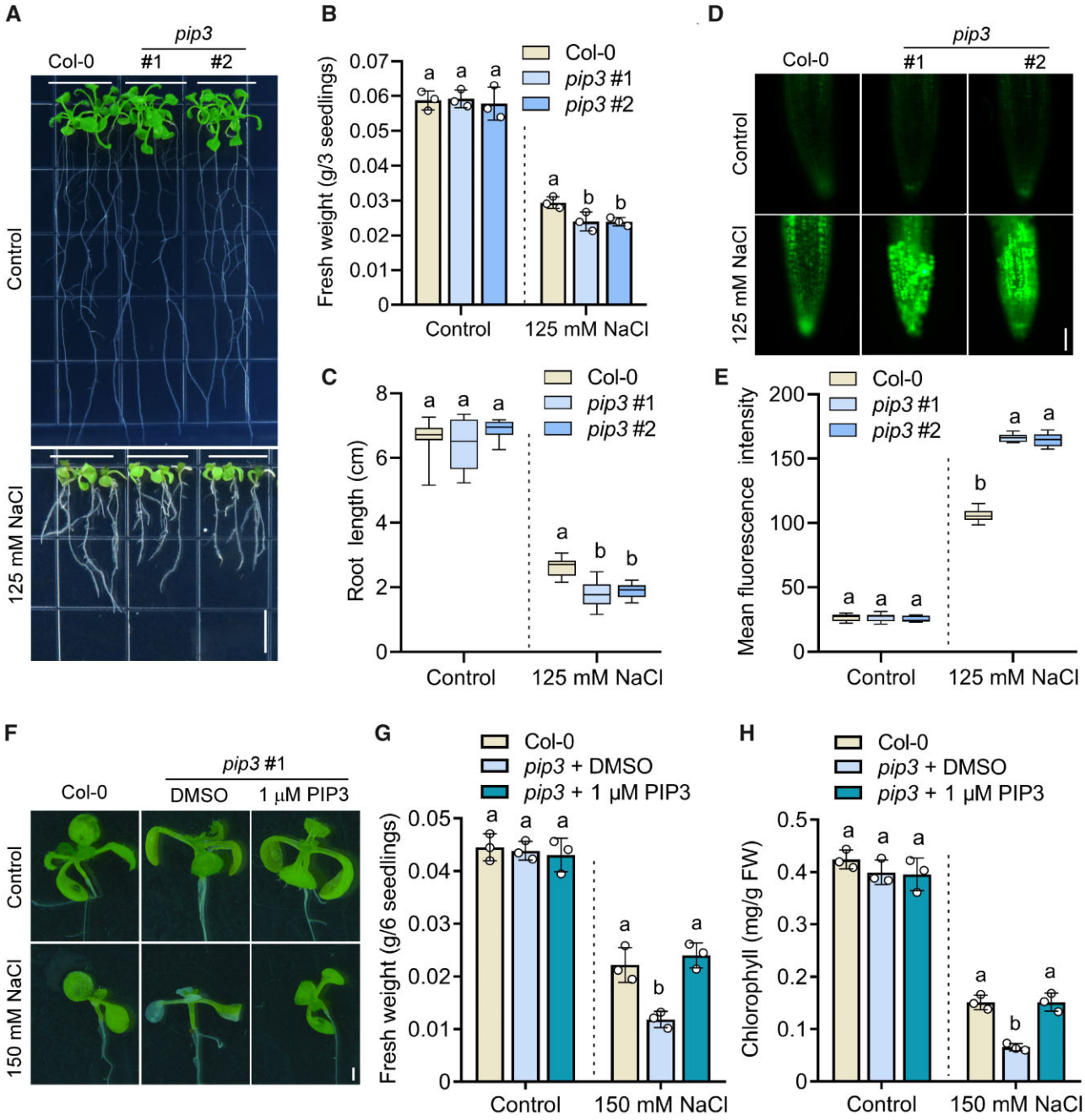

Figure 3 PIP3 functionally rescues the salt-sensitive phenotype of the *pip3* mutant. A, Salt sensitivity analysis. Four-day-old Col-0 and *pip3* seedlings were transferred to MS medium or MS medium containing 125-mM NaCl for additional growth, and the photographs were taken 7 days after transfer. Bar = 1 cm. B and C, Fresh weight (B) and root length (C) of seedlings in (A). Data are presented as means ± SD (n = 3 for [B] or n = 9 for [C]). Results are shown from three independent experiments. Different lowercase letters indicate a significant difference at $P < 0.05$ based on ANOVA. D, CoroNa Green staining. Seedlings of 4-day-old Col-0 and *pip3* left untreated or treated with 125-mM NaCl for 12 h were stained with CoroNa Green. Representative root tips are shown. Bar = 100 μm. E, Mean fluorescence intensity in (D). Data are presented as the means ± SDs (n = 9). Results are shown from three independent experiments. Different lowercase letters indicate a significant difference at $P < 0.05$ based on ANOVA. F, Synthetic PIP3 application and salt sensitivity analysis. Seedlings of Col-0 and *pip3* (line #1) were subjected to liquid culture-based salt sensitivity test with DMSO (solvent of PIP3) or 1 μM PIP3 treatment. Bar = 1 mm. G and H, Fresh weight (G) and chlorophyll contents (H) for seedlings in (F). Data are presented as means ± SD (n = 3). Results are shown from three independent experiments. Different lowercase letters indicate a significant difference at $P < 0.05$ based on ANOVA.

(Figure 4B). As a positive control, prePIP1-GST also interacted with Flag-tagged RLK7 in this pull-down system, although to a lower extent (Figure 4B). Considering that PIP3 can be secreted into the apoplastic space, we hypothesized that it might directly bind to the extracellular domain of RLK7. Using recombinant prePIP3-GST and a variety of truncated RLK7 proteins fused to a maltose-binding protein (MBP) tag (Figure 4C), we performed in vitro pull-down assays to

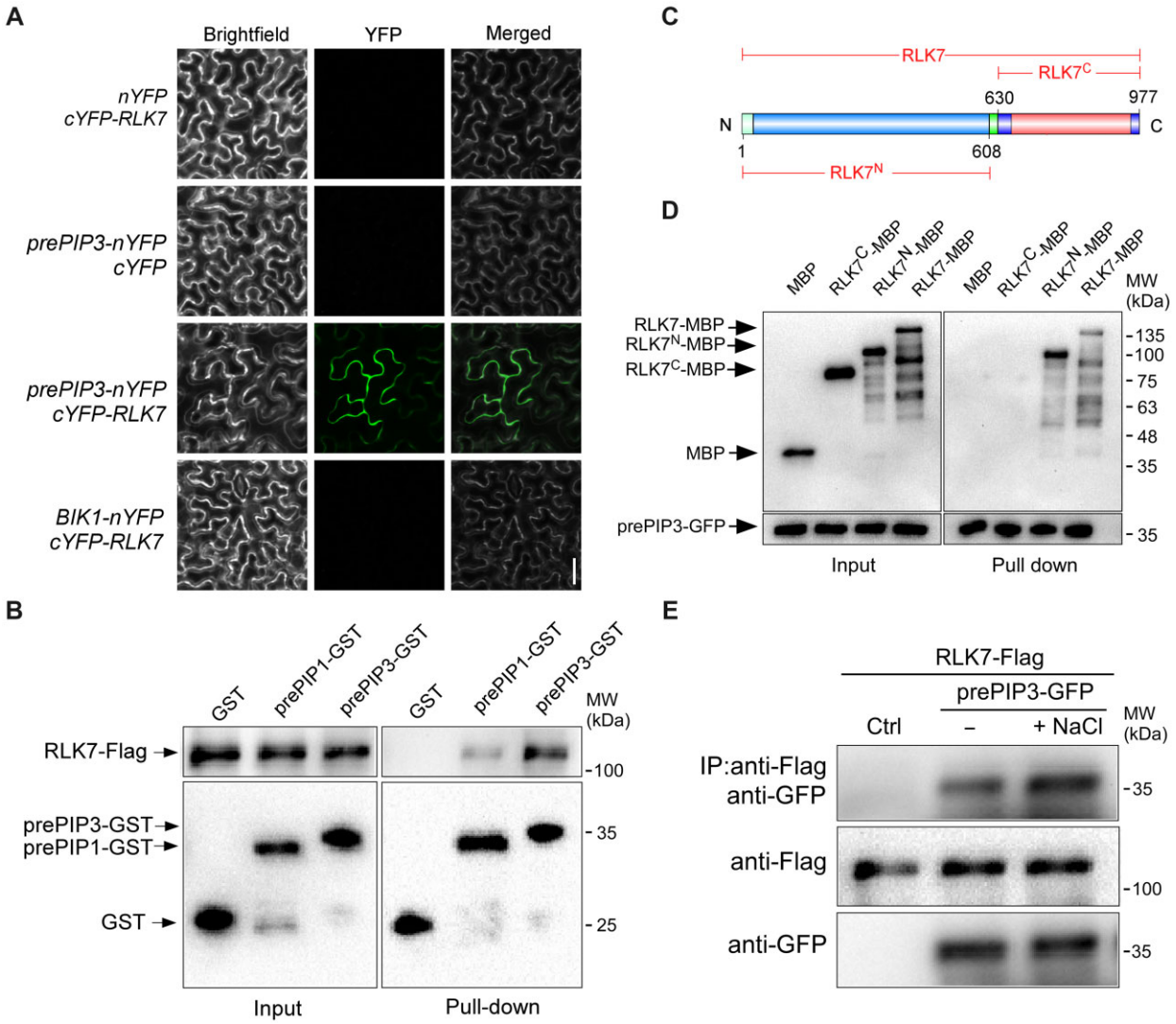

Figure 4 PIP3 interacts with RLK7. A, BiFC assay for PIP3 and RLK7 interaction in planta. The indicated constructs were transiently infiltrated in *N. benthamiana* leaves, and the YFP fluorescence signal was detected using a Leica SP5 confocal microscope. At least six randomly chosen regions of interest for each combination were examined and representative images are shown. Bar = 50 μm. B, Semi-in vivo pull-down assay. Recombinant prePIP3-GST or prePIP1-GST proteins purified from *Escherichia coli* (BL21) were incubated with protein extracts from *35Spro:RLK7-Flag* seedlings. GST or GST-tagged proteins were immunoprecipitated by Glutathione Sepharose, and the co-immunoprecipitated RLK7-Flag proteins were detected using anti-Flag antibody. C, Schematic structure of RLK7 protein and its truncated versions. $RLK7^{N}$, RLK7 N-terminus; $RLK7^{C}$, RLK7 C-terminus. D, In vitro pull-down assay. Recombinant RLK7-MBP, $RLK7^{N}$-MBP, or $RLK7^{C}$-MBP, prePIP3-GST, or GST protein alone was purified from *E. coli* (BL21). The resulting proteins were subjected to in vitro pull-down assay as described in Methods. $RLK7^{N}$, AA 1-608 of RLK7; $RLK7^{C}$, AA 630–977 of RLK7. E, Co-IP assay. Seedlings of *35Spro:RLK7-Flag 35Spro:prePIP3-GFP* and *35Spro:RLK7-Flag* were left untreated or treated with 125-mM NaCl for 3 h before Co-IP assay. RLK7-Flag proteins were immunoprecipitated with anti-Flag antibody-conjugated agarose and the RLK7-interacting prePIP3-GFP was detected using anti-GFP antibody. MW marker positions were added based on a comparison of the chemiluminescence blots to the original immunoblots.

delineate the interaction interface between PIP3 and RLK7. We first confirmed that full-length PIP3 and RLK7 physically interact each other. Notably, we determined that the extracellular domain rather than the intracellular region of RLK7 specifically binds PIP3 (Figure 4D). Finally, we tested whether the two proteins could be co-immunoprecipitated using protein extracts *35Spro:RLK7-Flag 35Spro:prePIP3-GFP* and *35Spro:RLK7-Flag* seedlings left untreated or treated with 125-mM NaCl. Indeed, prePIP3-GFP was co-immunoprecipitated with RLK7-Flag using anti-Flag antibody-conjugated agarose (Figure 4E). Importantly, the co-immunoprecipitation (Co-IP) assay revealed that salt stress significantly enhances PIP3–RLK7 binding affinity (Figure 4E). In contrast, although we also confirmed PIP1–RLK7 interaction by Co-IP assay, their binding affinity was not affected by salt stress (Supplemental Figure S6G). Taken together, these results demonstrated that PIP3 interacts with RLK7.

RLK7 is a mediator of plant salt tolerance

Next, we investigated whether RLK7 participated in plant salt tolerance in Arabidopsis. Relative *RLK7* transcript levels were highly induced by salt stress, as determined by RT-

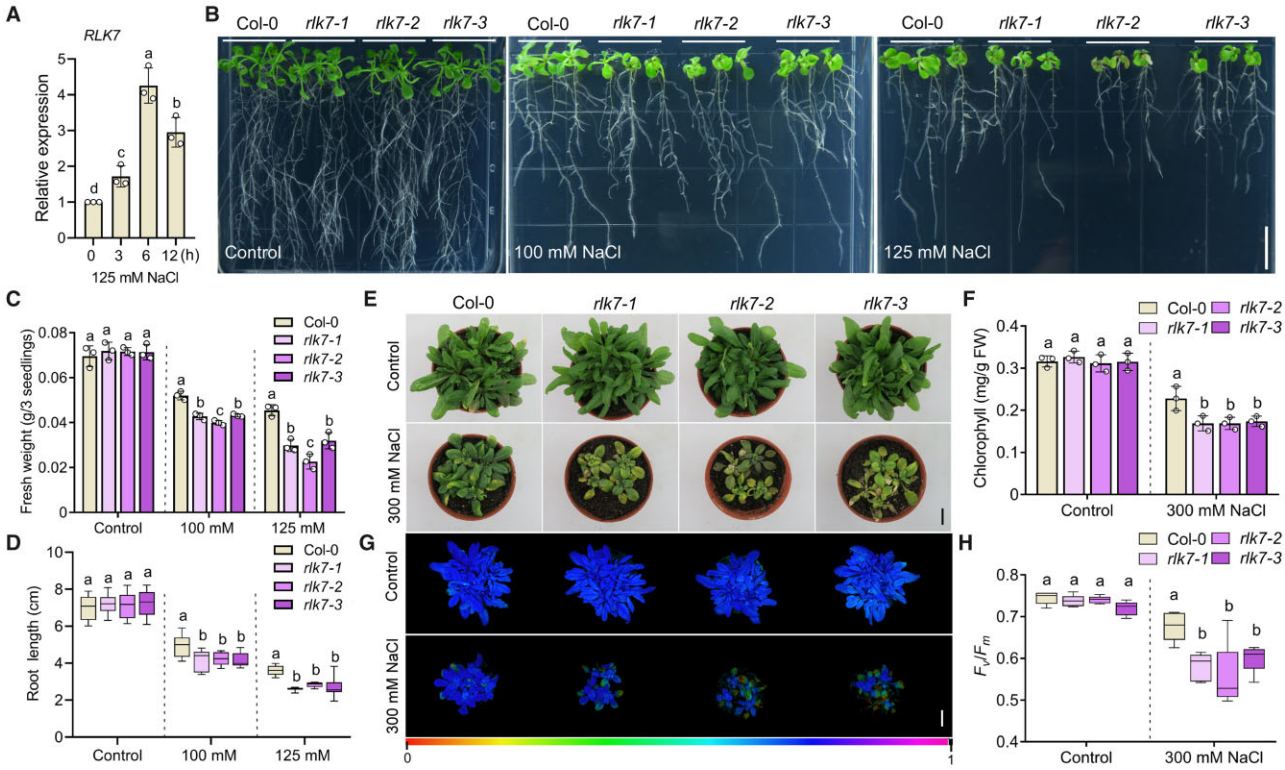

Figure 5 RLK7 functions in plant salt tolerance regulation. A, RT-qPCR analysis of *RLK7* transcript levels using 10-day-old Col-0 left untreated or treated with 125-mM NaCl for the indicated times. *ACTIN 2* was used as the internal control. Expression levels in Col-0 under control conditions were set to 1. Error bars represent SD ($n = 3$). Significant differences are indicated by different lowercase letters ($P < 0.05$), as determined by ANOVA. B, Salt sensitivity analysis. Four-day-old Col-0, *rlk7-1*, *rlk7-2*, and *rlk7-3* seedlings were transferred to MS medium or MS medium containing 100-mM or 125-mM NaCl for additional growth. Photographs were taken 7 days after transfer. Bar = 1 cm. C and D, Fresh weight (C) and root length (D) for seedlings in (A). Error bars represent SD ($n = 3$ for [C] or $n = 9$ for [D]). Results are shown from three independent experiments. Significant differences are indicated by different lowercase letters ($P < 0.05$), as determined by ANOVA. E, Salt sensitivity analysis of seedlings cultivated on soil. Two-week-old soil-grown Col-0, *rlk7-1*, *rlk7-2*, and *rlk7-3* seedlings were left untreated or treated with 300-mM NaCl for additional growth. Photographs were taken 7 days later. Bar = 1 cm. F, Chlorophyll contents for seedlings in (E). Error bars represent SD ($n = 3$). Results are shown from three independent experiments. Significant differences are indicated by different lowercase letters ($P < 0.05$), as determined by ANOVA. G, Chlorophyll fluorescence images of Col-0 and *rlk7* seedlings. Two-week-old soil-grown seedlings left untreated or treated with 300-mM NaCl for 7 days were used to determine chlorophyll fluorescence. The seedlings were dark-adapted for at least 30 min before imaging. Bar = 1 cm. H, Maximum photochemical activity of PSII (F_v/F_m) in (G). Error bars represent SD ($n = 6$). Results are shown from one representative out of three independent experiments. Significant differences are indicated by different lowercase letters ($P < 0.05$), as determined by ANOVA.

qPCR analysis, suggesting a possible role for RLK7 in plant salt response (Figure 5A). We identified three independent T-DNA insertional mutant lines in *RLK7* (*rlk7-1* to *rlk7-3*) for salt-sensitivity analyses (Supplemental Figure S8, A–C). When 4-day-old WT and *rlk7* mutant seedlings were transferred to MS medium without NaCl or MS medium containing various concentrations of NaCl for additional growth, the *rlk7* mutant seedlings showed much lower fresh weight and root length values than Col-0 under saline conditions, while we observed no obvious growth difference between the WT and mutant seedlings under control conditions (Figure 5, B–D). Furthermore, *rlk7* mutant seedlings accumulated more Na^+ but less K^+ ions compared to Col-0 under salt treatment (Supplemental Figure S9, A–H). Consistent with these results, soil-grown *rlk7* mutant plants exhibited severe growth inhibition with lower chlorophyll contents compared to Col-0 upon 300-mM NaCl treatment (Figure 5, E and F). When 2-week-old soil-grown Col-0 and *rlk7* mutant seedlings were left untreated or treated with 300-mM NaCl and subjected to measurement of their maximum photochemical efficiency of photosystem II (PSII), the F_v/F_m ratio decreased in both Col-0 and *rlk7* plants after salt exposure for 7 days, but was more pronounced in *rlk7* mutant plants than in Col-0, indicating that the mutant plants might suffer from severe photoinhibition under saline conditions due to the loss of RLK7 (Figure 5, G and H). Together, these results demonstrated that RLK7 is a functional mediator of plant salt tolerance in Arabidopsis.

PIP3 modulates plant salt tolerance in an RLK7-dependent manner

We explored the expression pattern of *PIP3* and *RLK7* by placing the β-*GLUCURONIDASE* (*GUS*) reporter gene under the control of the *prePIP3* or *RLK7* promoter and introducing the resulting constructs into the Col-0 background to generate *prePIP3pro:GUS* and *RLK7pro:GUS* transgenic lines.

We mainly detected the GUS staining pattern derived from the *prePIP3pro* in shoots under control conditions, but throughout the plant upon exposure to salt (Supplemental Figure S10A). Interestingly, *RLK7pro:GUS* produced a pattern similar to that of *prePIP3pro:GUS* (Supplemental Figure S10B). Therefore, the temporal and spatial coincidence of *prePIP3pro:GUS* and *RLK7pro:GUS* distributions suggested that PIP3 and RLK7 may function in a common signaling module during salt stress response.

We asked whether PIP3 triggered salt tolerance through RLK7 in Arabidopsis. To this end, we treated 7-day-old Col-0 and *rlk7-2* mutant seedlings with synthetic PIP3 peptide using the liquid culture-based salt sensitivity assay. We determined that exogenous application of PIP3 peptide substantially improves salt tolerance of Col-0 but not *rlk7-2* plants (Figure 6, A and B). The chlorophyll contents of Col-0 seedlings treated with PIP3 were much higher than those treated with dimethyl sulfoxide (DMSO, used as solvent for PIP3) under saline conditions; however, the chlorophyll contents in *rlk7-2* seedlings remained low whether treated with PIP3 or DMSO upon salt exposure (Figure 6C). We also generated independent *rlk7-2 35Spro:prePIP3-GFP* transgenic lines (*rlk7-2 PIP3-OX*, lines #1 and #2) for salt sensitivity assays (Supplemental Figure S7B). When Col-0, *rlk7-2*, *PIP3-OX*, and *rlk7-2 PIP3-OX* seedlings were transferred from MS medium to fresh MS medium containing 125-mM NaCl for additional growth, we discovered that the enhanced salt resistance in *PIP3-OX* plants compared to Col-0 is nearly abolished in *rlk7-2 PIP3-OX* plants, while *rlk7-2* and *rlk7-2 PIP3-OX* seedlings exhibited comparable salt sensitivity (Figure 6, D–F), suggesting that RLK7 functions downstream of PIP3 in plant salt tolerance signaling. Taken together, these data demonstrated that PIP3 modulates salt tolerance through RLK7 in Arabidopsis.

Salt stress induces RLK7 phosphorylation via the action of PIP3

RLK7 is a typical PM-localized LRR-RLK (Supplemental Figure S8D), prompting us to ask whether the phosphorylation status of RLK7 was altered upon salt exposure. When *35Spro:RLK7-GFP* (*RLK7-OX*, lines #13 and #20) seedlings (Supplemental Figure S7C) were left untreated or treated with 125-mM NaCl for the indicated time periods, we observed an increase in the abundance of a slower migrating RLK7 form, and treating the samples with shrimp alkaline phosphatase (rSAP) largely abolished the accumulation of this band (Figure 7A; Supplemental Figure S11A), indicating that salt stress significantly induces RLK7 phosphorylation, which may represent the activation of RLK7 in response to salt stress. Since PIP3 was a possible RLK7 ligand, we asked whether exogenous PIP3 application would also increase RLK7 phosphorylation. Indeed, RLK7 phosphorylation was significantly increased by exogenous treatment of PIP3 but not DMSO (Figure 7B; Supplemental Figure S11B). Furthermore, two independent transgenic lines *pip3 35Spro:RLK7-GFP* (*pip3 RLK7-OX*, lines #1 and #2) were used to determine RLK7 phosphorylation status in the *pip3* mutant background (Supplemental Figure S7C). RLK7 phosphorylation decreased strongly in response to salt stress in *pip3 RLK7-OX* plants compared to *RLK7-OX* plants (Figure 7C; Supplemental Figure S11C). We transferred Col-0, *rlk7-2*, *RLK7-OX*, and *pip3 RLK7-OX* seedlings from MS medium to MS medium containing no NaCl or with 125-mM NaCl for additional growth. Under salt conditions, *RLK7-OX* plants exhibited enhanced salt tolerance compared to WT plants, but this enhancement was largely abolished in *pip3 RLK7-OX* plants (Figure 7, D–F). Taken together, these results demonstrated that the PIP3 peptide ligand mediates RLK7 activation for plant salt tolerance.

PIP3–RLK7 module regulates salt tolerance by activating MPK3/6

MPK3 and MPK6 are versatile downstream effectors mediating signal transduction in response to multiple stresses (Li et al., 2014; Zhao et al., 2017). To examine whether the MPK3/MPK6 cascades were involved in salt tolerance regulation mediated by the PIP3–RLK7 module, we determined the activation of MPK3/6 in Col-0 and *rlk7-2* seedlings upon salt exposure using phospho-p44/42 MAPK antibodies, as previously described (Zhao et al., 2017). MPK3/6 phosphorylation did significantly increase in Col-0 but not in *rlk7-2* mutant treated with salt (Figure 8A). We next wished to assess the functional role of PIP3 in salt stress-induced MPK3/6 activation. To this end, we treated Col-0 and *rlk7-2* seedlings with 1-μM synthetic PIP3 peptide for the indicated time periods and determined the phosphorylation status of MPK3/6. Exogenous application of synthetic PIP3 peptide significantly enhanced MPK3/6 activation in Col-0 but not in *rlk7-2* (Figure 8B). In agreement, when Col-0 and *pip3* (line #1) seedlings were treated with 125-mM NaCl, the salt-induced activation of MPK3/6 was significantly attenuated in *pip3* seedlings relative to Col-0 (Figure 8C). These results demonstrated that the PIP3–RLK7 module activates MPK3/6 signaling in response to salt stress.

To further examine the regulatory role of MPK3/6 in plant salt tolerance mediated by the PIP3–RLK7 module, we crossed *mpk3-1* and *mpk6-2* with *PIP3-OX* plants to generate *mpk3-1 35Spro:prePIP3-GFP* (*mpk3-1 PIP3-OX*) and *mpk6-2 35Spro:prePIP3-GFP* (*mpk6-2 PIP3-OX*) lines for salt sensitivity analyses (Supplemental Figure S7D). We found that *mpk3-1 PIP3-OX* and *mpk6-2 PIP3-OX* plants exhibit a salt-sensitive phenotype comparable to that of *mpk3-1* and *mpk6-2*, whereas the salt resistance in *PIP3-OX* significantly increased compared to Col-0 due to *PIP3* overexpression (Figure 8, D–F), suggesting that the salt tolerance mediated by PIP3 peptide is dependent on MPK3/6. We also generated *mpk3-1 35Spro:RLK7-GFP* (*mpk3-1 RLK7-OX*) and *mpk6-2 35Spro:RLK7-GFP* (*mpk6-2 RLK7-OX*) plants (Supplemental Figure 7E). Again, we failed to observe the elevated fresh weight and root length seen in *RLK7-OX* plants compared to Col-0 grown under saline conditions in *mpk3-1 RLK7-OX* and *mpk6-2 RLK7-OX* plants compared to *mpk3-1* and

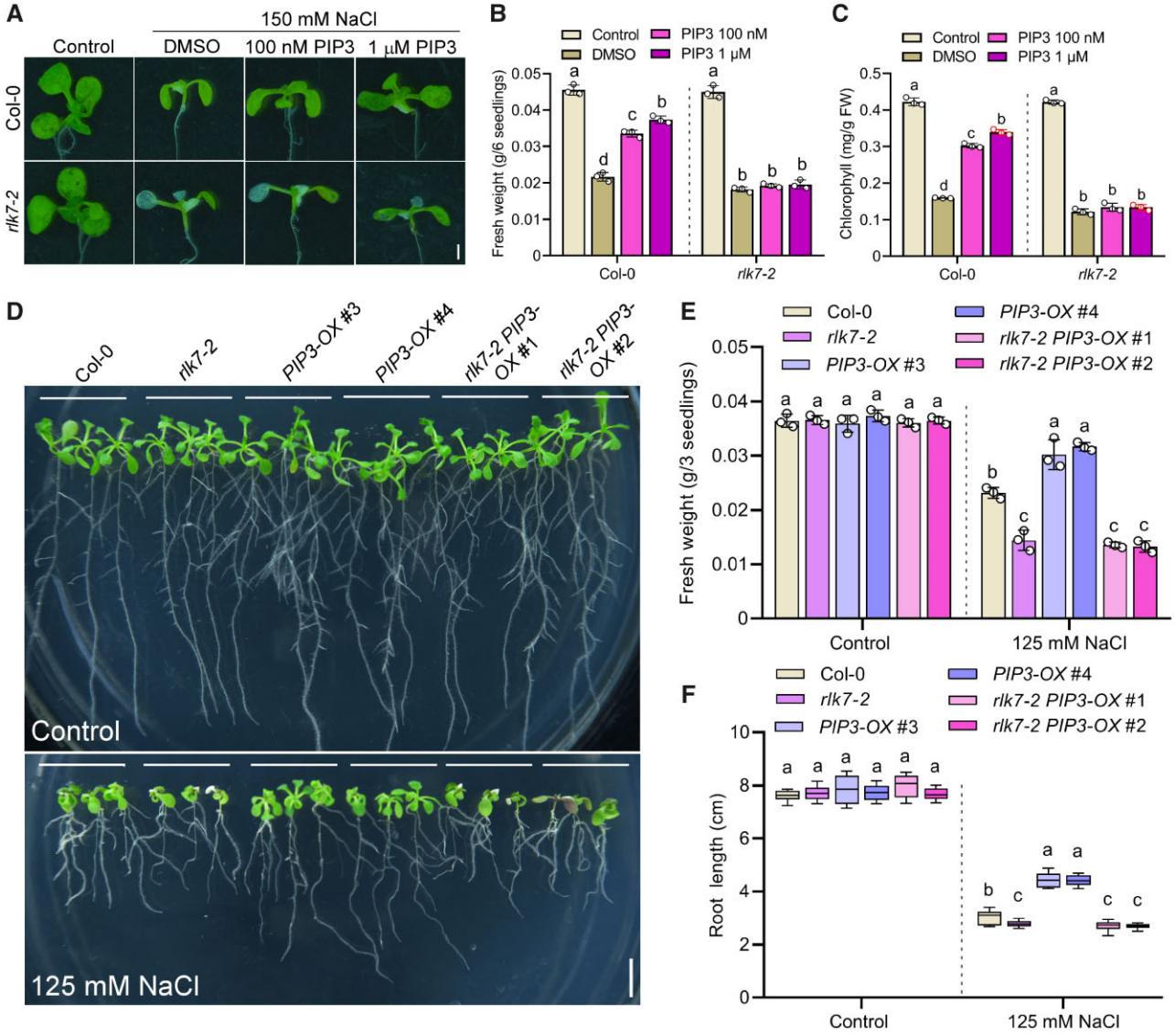

Figure 6 PIP3 activates plant salt tolerance through RLK7. A, Phenotypic analysis of plant salt sensitivity. Col-0 and *rlk7-2* seedlings were subjected to liquid culture-based salt stress assays with application of DMSO or PIP3 peptide at the indicated concentrations at 23°C for 7 days. Images were taken and chlorophyll contents and fresh weight were measured. Bar = 1 mm. B and C, Fresh weight (B) and chlorophyll contents (C) for seedlings in (A). Error bars represent SD ($n = 3$). Results are shown from three independent experiments. Significant differences are indicated by different lowercase letters ($P < 0.05$), as determined by ANOVA. D, Phenotypic analysis of plant salt sensitivity. Four-day-old Col-0, *rlk7-2*, and *PIP3-OX* (lines #3 and #4) and *rlk7-2 35Spro:prePIP3-GFP* (*rlk7-2 PIP3-OX*, lines #1 and #2) seedlings were transferred to MS medium or MS medium containing 125-mM NaCl for additional growth. Photographs were taken 7 days after transfer. E and F, Fresh weight (E) and root length (F) for the seedlings in (D). Error bars represent SD ($n = 3$ for [E] or $n = 9$ for [F]). Results are shown from three independent experiments. Significant differences are indicated by different lowercase letters ($P < 0.05$), as determined by ANOVA.

mpk6-2, respectively (Figure 8, G–I). Taken together, we concluded that MPK3 and MPK6 function downstream of the PIP3–RLK7 module, leading to enhanced salt tolerance in plants.

Discussion

Various small peptides encoded by short genes have been identified in plants (Matsubayashi, 2001; 2014); however, only a few have been functionally annotated or reported to function in abiotic stress tolerance. In this study, we report that the peptide ligand PIP3 modulates plant salt tolerance by activating its possible receptor RLK7 in Arabidopsis, and that the MPK3/6 signaling cascade acts as essential downstream components of the PIP3–RLK7 module to trigger salt tolerance (Figure 9).

We found that *prePIP3* expression is salt stress-induced and that overexpression of *prePIP3* significantly improves salt tolerance in Arabidopsis, possibly by re-establishing cellular ionic homeostasis. Conversely, the PIP3 loss-of-function mutant *pip3* exhibited a severe salt-sensitive phenotype. Application of synthetic PIP3 peptide to WT plants recapitulated the salt-tolerant phenotype of *PIP3-OX* seedlings. The

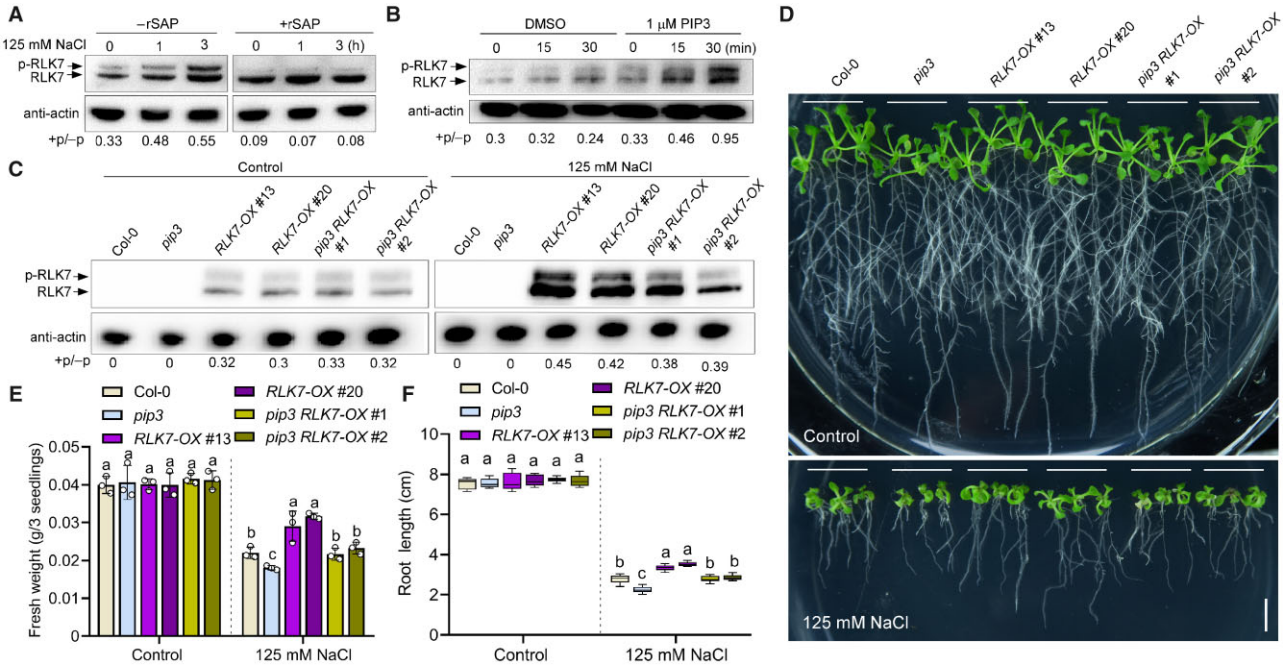

Figure 7 Salt stress induces RLK7 phosphorylation via the action of PIP3, leading to enhanced salt tolerance. A, Determination of the phosphorylation status of RLK7. Total protein extracts from 10-day-old *35Spro:RLK7-GFP* seedlings left untreated or treated with 125-mM NaCl for the indicated periods of time were incubated with or without rSAP. The phosphorylation status of RLK7 was determined by immunoblot analysis using anti-GFP antibody. Results are shown from one representative out of three independent experiments. Numbers below blots represent the ratio of phosphorylated RLK7 to nonphosphorylated RLK7 (+ p/−p). B, PIP3 peptide enhances RLK7 phosphorylation. Total proteins were extracted from 10-day-old *35Spro:RLK7-GFP* seedlings treated with 1-μM PIP3 or an equal volume of DMSO for immunoblot analysis using anti-GFP antibody. Results are shown from one representative out of three independent experiments. Numbers below blots represent the ratio between phosphorylated RLK7 and nonphosphorylated RLK7 (+ p/−p). C, Genetic inactivation of *PIP3* attenuates salt-induced phosphorylation of RLK7. Total protein extracts from 10-day-old Col-0, *pip3*, *35Spro:RLK7-GFP* (*RLK7-OX*, lines #13 and #20) and *pip3 35Spro:RLK7-GFP* (*pip3 RLK7-OX*, lines #1 and #2) seedlings left untreated or treated with 125-mM NaCl were subjected to immunoblot analysis using anti-GFP antibody. Results are shown from one representative out of three independent experiments. Numbers below blots represent the ratio of phosphorylated RLK7 to nonphosphorylated RLK7 (+ p/−p). D, Phenotypic analysis of plant salt sensitivity of Col-0, *pip3*, *RLK7-OX* (lines #13 and #20), and *pip3 RLK7-OX* (lines #1 and #2). Four-day-old seedlings were transferred to MS medium or MS medium containing 125-mM NaCl for additional growth. Photographs were taken 7 days after transfer. Bar = 1 cm. E and F, Fresh weight (E) and root length (F) for seedlings in (D). Error bars represent ± SDS ($n = 3$ for [E] or $n = 9$ for [F]). Results are shown from three independent experiments. Significant differences are indicated by different lowercase letters ($P < 0.05$), as determined by ANOVA.

findings presented here have expanded the biological functions of the PIP/PIPL peptide family. Using BiFC assays, we tested several hypothetical PIP3 receptors and identified a member of class XI LRR-RLKs as a candidate. RLK7 is a typical PM-localized RLK whose extracellular N terminus physically interacts with PIP3. In fact, the N-terminal domain of the RLK7 extracellular region was reported to bind specific ligands, making RLK7 a potential sensor from environmental stimuli (Pitorre et al., 2010; Hou et al., 2014). In addition, PIP3-mediated salt tolerance functioned in an RLK7-dependent manner. Phosphorylation is a representative hallmark of RLK activation, which plays an essential role in transmitting various signals in response to environmental stimuli (Shiu et al., 2004; Macho et al., 2015; Chen et al., 2016). In our work, we observed the rapid phosphorylation/activation of RLK7 upon salt exposure; importantly, the PIP3 peptide ligand was involved in RLK7 activation. The genetic inactivation of PIP3 significantly attenuated RLK7 phosphorylation under saline conditions, leading to decreased salt tolerance. It is thus possible that RLK7 may sense salt stress via the action of the PIP3 ligand. The salt-induced accumulation of PIP3 would thus mediate salt tolerance by interacting with and activating RLK7; therefore, PIP3 and RLK7 may form a functional module for plant salt tolerance regulation. It should be noted that although we detected direct physical interaction between PIP3 and RLK7, we cannot exclude the possibility that PIP3-mediated RLK7 activation also requires additional components in planta. Additional biochemical assays should be performed to answer this question. Importantly, our data showed that both *PIP3* and *RLK7* are mainly expressed in shoots under control conditions, but became expressed throughout the entire plant in response to salt stress. Considering that PIP3 or RLK7 loss-of-function affects the salt resistance of plants both in their shoot and root parts, we speculate that the PIP3–RLK7 module may be implicated in local signaling during plant salt responses. However, whether PIP3 functions as a

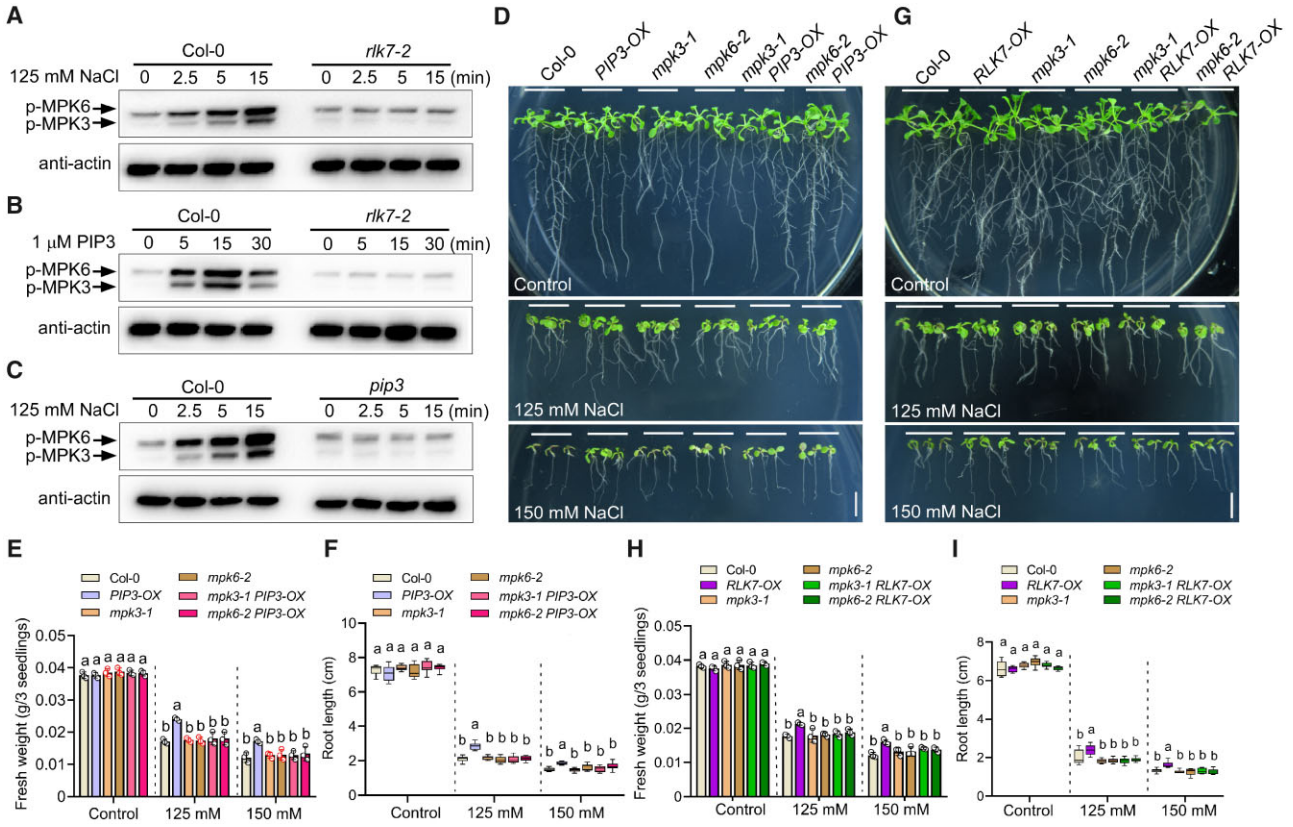

Figure 8 PIP3–RLK7 module regulates salt tolerance by activating MPK3/6. A, Determination of the activation of MPK3/6 in seedlings in response to salt stress. Ten-day-old Col-0 and *rlk7-2* seedlings were left untreated or treated with 125-mM NaCl for indicated time period (2.5, 5, or 15 min). Immunoblot analysis using the phospho-p44/42 MAPK antibody was conducted. Results are shown from one representative out of three independent experiments. B, Determination of the activation of MPK3/6 in seedlings with PIP3 treatment. Ten-day-old Col-0 and *rlk7-2* seedlings were left untreated or treated with 1 μM synthetic PIP3 for indicated time period (5, 15, or 30 min). Immunoblot analysis using the phospho-p44/42 MAPK antibody was conducted. Results are shown from one representative out of three independent experiments. C, The *pip3* mutant inhibits MPK3/6 activation upon salt exposure. Ten-day-old Col-0 and *pip3* seedlings were left untreated or treated with 125-mM NaCl for the indicated times (2.5, 5, or 15 min). Immunoblot analysis using the phospho-p44/42 MAPK antibody was conducted. Results are shown from one representative out of three independent experiments. D, Salt sensitivity analysis. Four-day-old Col-0, *PIP3-OX*, *mpk3-1*, *mpk6-2*, *mpk3-1 35Spro:prePIP3-GFP* (*mpk3-1 PIP3-OX*), and *mpk6-2 35Spro:prePIP3-GFP* (*mpk6-2 PIP3-OX*) seedlings were transferred to MS medium without (Control) or with 125- or 150-mM NaCl for additional growth. Photographs were taken 7 days after transferring. Bar = 1 cm. E and F, Fresh weight (E) and root length (F) for seedlings in (D). Error bars represent SD (n = 3 for [E] or n = 9 for [F]). Results are shown from three independent experiments. Significant differences are indicated by different lowercase letters ($P < 0.05$), as determined by ANOVA. G, Salt sensitivity analysis. Four-day-old Col-0, *RLK7-OX*, *mpk3-1*, *mpk6-2*, *mpk3-1 35Spro::RLK7-GFP* (*mpk3-1 RLK7-OX*), and *mpk6-2 35Spro:RLK7-GFP* (*mpk6-2 RLK7-OX*) seedlings were transferred to MS medium without (Control) or with 125 or 150-mM NaCl for further growth. Photographs were taken 7 days after transfer. Bar = 1 cm. H and I, Fresh weight (H) and root length (I) for seedlings in (G). Error bars represent SD (n = 3 for [H] or n = 9 for [I]). Results are shown from three independent experiments. Significant differences are indicated by different lowercase letters ($P < 0.05$), as determined by ANOVA.

possible long distant signal during initial salt response signaling should be investigated in the future.

RLK7 may be activated by various PIP/PIPL members (Hou et al., 2014; Toyokura et al., 2019) or other extracellular ligands (Matsubayashi and Sakagami, 2006; Shinohara et al., 2012; Hohmann et al., 2017) for growth or stress response regulation. In our study, PIP3 rather than PIP1 exerted a regulatory role in plant salt tolerance through RLK7, although the accumulation of both peptides was salt-induced and both formed a complex with RLK7. Considering that small peptides can undergo multiple posttranslational modifications (PTMs) during processing, such PTMs might explain the functional difference between PIP3 and PIP1 in plant salt tolerance regulation. Whether specific PTMs are added onto PIP3 in response to salt stress should be tested in the future, as well as the functional link between these PTMs and RLK7 activation and plant salt tolerance. Possible RLK7 co-receptors or other regulatory components might be also involved in specifying the interactions between RLK7 and its ligands, leading to fine-tuned downstream signaling for proper response to multiple endogenous or environmental stimuli. Characterization of such regulators in the PIP3–RLK7 module will be important. Notably, more than one peptide–receptor pair has been identified for plant salt tolerance regulation (Nakaminami et al., 2018; Zhao et al., 2018), raising the possibility that these signaling pathways

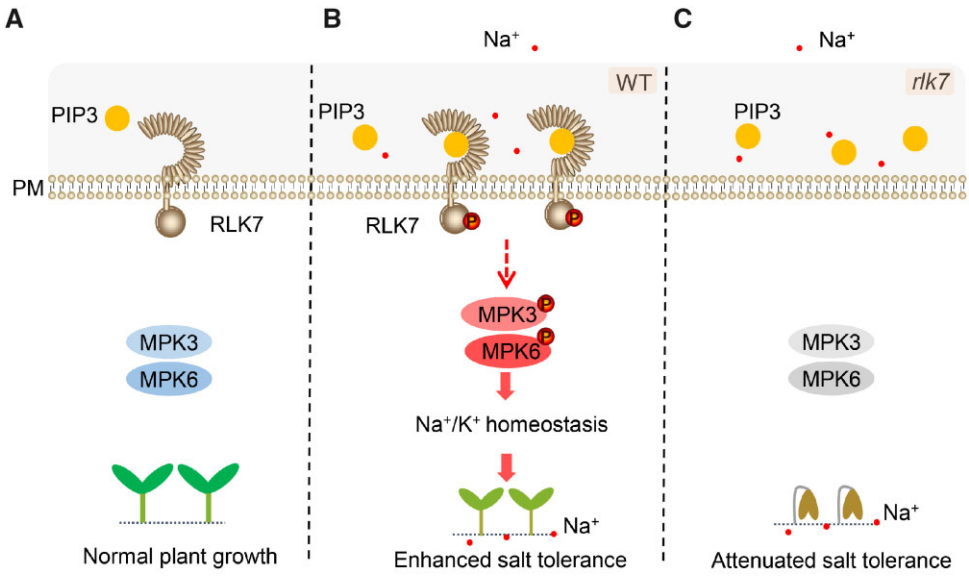

Figure 9 A working model for PIP3–RLK7 module-mediated salt tolerance. A, In WT seedlings grown under normal growth conditions, the PIP3 peptide accumulates to basal levels, while RLK7 and downstream MPK3/6 are inactive. Therefore, seedlings exhibit normal growth. B and C, In WT seedlings, both PIP3 and RLK7 accumulate to high levels upon salt exposure. PIP3–RLK7 interaction results in RLK7 activation, leading to the activation of MPK3/6 for salt stress signal amplification. Therefore, cellular ionic homeostasis is restored under saline conditions, resulting in enhanced salt tolerance (B). In *rlk7* mutant seedlings, PIP3–RLK7 module is disrupted due to RLK7 loss-of-function, leading to attenuated salt tolerance and repressed plant survival (C). *rlk7*, RLK7 loss-of-function mutant.

may coordinately modulate plant salt tolerance: various ligand–receptor modules might be activated in different tissues or at different times upon salt exposure, ensuring full stress response for downstream signaling initiation. The downstream components of each signaling pathway might be functionally linked or even shared, therefore amplifying stress signaling for fine-tuned plant growth in response to salt stress. Whether the PIP3–RLK7 module cross-talks with other signaling pathways underlying plant salt tolerance should be explored in the future.

MAPK cascades are conserved in eukaryotes (Mishra et al., 2006). Upon perception of environmental stimuli, MAP3K, MAP2K, and MAPK can be sequentially phosphorylated, leading to sequential phosphorelay in plants (Mishra et al., 2006; Cristina et al., 2010). For instance, MPK3/6 are activated by cold (Zhao et al., 2017), heat (Evrard et al., 2013), and salt (Yu et al., 2010), to connect phytohormonal signals and second messengers such as Ca^{2+} and ROS in Arabidopsis (Droillard et al., 2002; Chang et al., 2012; Smékalová et al., 2014). Besides the upstream MAPK kinases, MAPKs are also activated by other kinases (Moon et al., 2003; Takahashi et al., 2011; Li et al., 2014). In this study, our genetic and biochemical evidence revealed that the PIP3–RLK7 module may transmit salt response signals by activating MPK3/6 in Arabidopsis. Loss-of-function of RLK7 or PIP3 impaired salt-induced MPK3/6 activation, and the PIP3 peptide ligand enhanced MPK3/6 activation in WT but not in the *rlk7-2* mutant. Salt sensitivity analyses confirmed that the PIP3–RLK7 signaling cascade-mediated salt tolerance is dependent on MPK3/6. Our data suggest that RLK7 activated by PIP3 transmits the salt stress signal to MPK3/6 directly or to other unknown components to activate MPK3/6, resulting in enhanced salt tolerance. Further studies are required to verify the possible immediate downstream elements of the PIP3–RLK7 module for MPK3/6 activation.

Taken together, our work characterizes the small peptide ligand PIP3 as an interactor and activator of RLK7, therefore amplifying salt response signaling possibly via the action of MPK3/6 for plant resistance to salt stress (Figure 9). The findings presented here provide a better understanding of how plants respond and adapt to salt stress, and offer putative targets for the construction of salt-tolerant crops in the future.

Materials and methods

Plant materials

Homozygous *pip3* mutants were constructed using CRISPR/Cas9 gene editing as described (Li et al., 2020). The T-DNA insertional mutants *rlk7-1* (SALK_056583), *rlk7-2* (SALK_083114), and *rlk7-3* (SALK_120595), were obtained from the Arabidopsis Biological Resource Center. Both *mpk3-1* and *mpk6-2* mutants were kindly provided by Dr Juan Xu from Zhejiang University. The transgenic plants *35Spro:RLK7-GFP* and *35Spro:prePIP3-GFP* were generated as described below in methods. Subsequently, the mutants *mpk3-1*, *mpk6-2*, or *pip3* were crossed to the transgenic lines *35Spro:RLK7-GFP* to generate *mpk3-1 35Spro:RLK7-GFP*, *mpk6-2 35Spro:RLK7-GFP*, or *pip3 35Spro:RLK7-GFP*, respectively. The mutants *mpk3-1*, *mpk6-2*, or *rlk7-2* were crossed to the transgenic line *35Spro:prePIP3-GFP* to generate *mpk3-1 35Spro:prePIP3-GFP*, *mpk6-2 pro35S:prePIP3-GFP* or *rlk7-2 pro35S:prePIP3-GFP*, respectively. For each construct, more

than 12 independent lines were obtained, and representative T_2 lines were used for subsequent analyses except *35Spro:prePIP3-GFP*, for which three independent T_2 lines (#3, #4, and #6) were used.

Construction of homozygous *pip3* mutants

For the construction of *pip3* mutants, two sgRNAs targeting *prePIP3* 75 bp (sgRNA1: 5′-TCGTCCTTTGGGTTTAACGA AGG-3′) and 139 bp (sgRNA2: 5′-CTTGGGGCGATTAAGGA GTCGGG-3′) downstream of the translation initiation codon (ATG) were designed using an online CRISPR/Cas9 target predictor (http://crispr.cos.uni-heidelberg.de/). Two *U6* promoter-sgRNA-*U6* terminator cassettes were amplified by PCR using vector pCBC-DT1T2 as the template; the PCR fragments were then cloned into the pHEC401 vector as described previously (Wang et al., 2015). The resulting constructs were introduced into the Col-0 accession by Agrobacterium (*Agrobacterium tumefaciens*, strain EHA105)-mediated transformation. Genomic sequences from hygromycin-resistant transgenic plants that contain the sgRNA target sites were amplified using primer sets shown in Supplemental Table S1; the amplicons were sequenced to ascertain the presence of the desired mutations at the target regions. Two independent *pip3* mutants (lines #1 and #2) harboring the same 47-bp deletion in the *prePIP3* gene were identified.

Plant growth and salt sensitivity analysis

Mature seeds were surface sterilized using a solution containing 20% (w/v) Na hypochlorite and 0.1% (v/v) Triton X-100 for 15 min, washed 5 times with sterile water, and sown on MS medium (pH 5.8, containing 2.5% [w/v] sucrose and 0.3% [w/v] phytagel agar, Sigma-Aldrich, St Louis, MO, USA). Plates were kept at 4°C for 2 days, and then seeds were germinated and grown under constant illumination (100 µmol m^{-2} s^{-1}; 16-h light/8-h dark) at 23°C.

For salt sensitivity assays on plates, Arabidopsis Col-0 (WT), mutants, or related transgenic plants were germinated and grown vertically on MS medium for 4 days. Then, seedlings were transferred to MS medium with or without 100-, 125-, or 150-mM NaCl. Photographs were taken 7 days after transfer. Root length and fresh weight were scored. For salt sensitivity assays in soil, 2-week-old seedlings of WT, mutants, or related transgenic plants were subjected to control (no NaCl added) or 300-mM NaCl treatment for 7 days. Photographs were taken and chlorophyll content was determined. For each experiment, at least three replicates were performed and similar results were obtained.

The liquid culture-based salt sensitivity assays were performed as previously described, with minor modifications (Nakaminami et al., 2018). Briefly, WT, *rlk7-2*, or *pip3* seedlings were grown in liquid MS medium for 7 days at 23°C under long-day conditions (16-h light/8-h dark). Salt stress tests were then carried out by replacing the liquid medium with new medium containing 150-mM NaCl. The seedlings were grown at 23°C for another 7 days and salt sensitivity was subsequently evaluated by measuring the chlorophyll content and fresh weight of the tested plants.

Peptide design and treatment assay

PIP3 and PIP1 synthetic peptides were synthesized by and purchased from GL Biochem (Shanghai, China); the peptide information is summarized in Supplemental Table S3. The synthetic peptides were dissolved in DMSO and peptide treatment was performed following the liquid culture-based salt sensitivity assay. WT or relevant mutant seedlings were cultivated in liquid MS medium for 4 days. The medium was then replaced by MS medium containing PIP3 peptide or PIP1 peptide; seedlings were grown for 3 days to serve as a peptide pretreatment. The salt sensitivity assays were performed by replacing the peptide-containing medium with MS medium containing 150-mM NaCl with PIP3 peptide, PIP1 peptide, or DMSO (Control) after the pretreatment. The seedlings were grown for another 7 days at 23°C, and images were taken and the chlorophyll content was determined.

Subcellular protein localization

The coding sequences of *RLK7* and *prePIP3* were amplified with the LP-*RLK7*-GFP/RP-*RLK7*-GFP, and LP-*prePIP3*-GFP/RP-*prePIP3*-GFP primer pairs and cloned into the p1300-GFP vector using the SalI and KpnI sites, respectively. The resulting constructs were then introduced into Agrobacterium infiltrated into *N. benthamiana* leaves. Infiltrated leaves were returned to normal growth conditions for 2 days, and the fluorescent signals were then visualized under Leica SP5 microscope. For PIP3 subcellular localization analysis, epidermal cells of *N. benthamiana* leaves were first subjected to plasmolysis in 1 M mannitol treatment for 30 min before microscopy. To mark the PM, aquaporin PIP2;1 was fused to mCherry (Ma et al., 2015) and transiently infiltrated in *N. benthamiana* leaves along with *prePIP3-GFP*. For the subcellular localization of RLK7, the PM-specific dye FM4-64 (Invitrogen, Waltham, MA, USA; CD4673) was used as described (Tian et al., 2015). Sequences of primers used for plasmids construction can be found in Supplemental Table S1.

In vitro pull-down assays

Full length or truncated RLK7 ($RLK7^N$ or $RLK7^C$) were fused to an MBP tag by cloning the cloning sequences into the pMAL-C2X vector, while full-length prePIP3 was fused to a GST tag by cloning into the pGEX-4T-1 vector. Recombinant GST-tagged prePIP3 or GST were purified with glutathione Sepharose (GE Healthcare, Chicago, IL, USA; 17-0756-05) according to the manufacturer's protocol, while MBP-tagged RLK7, $RLK7^N$, and $RLK7^C$ proteins were purified with Amylose resin (NEB, E8021S, Ipswich, MA, USA). Subsequently, 5 µg recombinant prePIP3-GST proteins were incubated with 5 µg recombinant RLK7-MBP, $RLK7^N$-MBP, $RLK7^C$-MBP, or MBP in 500 µL pull-down buffer (150-mM NaCl, 20-mM Tris–HCl [pH 8.0], 1-mM PMSF, 0.2% [v/v] Triton X-100, and 1% [w/v] protease inhibitor cocktail) at

4°C for 2 h. Glutathione Sepharose beads were washed thoroughly with pull-down buffer and proteins were eluted from beads by boiling at 95°C with 30 μL sodium dodecyl sulfate–polyacrylamide gel electrophoresis (SDS–PAGE) loading buffer for 10 min. The samples were then separated by SDS–PAGE and analyzed by the anti-MBP (NEB, E8032S) and anti-GST (BioEasy, Shenzhen, China; BE2013) antibodies. Sequences of primers used for plasmids construction can be found in Supplemental Table S1.

BiFC assays

To determine the interaction between RLK7 and PIP3 in planta, the coding sequence of *prePIP3* was cloned into the pXY103 vector (nYFP), while the coding sequence of *RLK7* was cloned into the pXY104 (cYFP) vector. The resulting constructs were introduced into Agrobacterium strain EHA105 by electroporation and infiltrated into *N. benthamiana* leaves. As negative control, *prePIP3-nYFP* and *cYFP*, *RLK7-cYFP*, and *nYFP*, as well as *BIK1-nYFP* and *RLK7-cYFP*, were co-infiltrated in *N. benthamiana* leaves, respectively. Three days after infiltration, YFP fluorescence was detected using a Leica SP5 confocal microscope. Three independent experiments were performed and similar results were obtained. Sequences of primers used for plasmids construction can be found in Supplemental Table S1.

Co-IP assays

The Co-IP assays were performed as previously described (Zhou et al., 2012). Briefly, total proteins from transgenic plants *35Spro:RLK7-Flag 35Spro:prePIP3-GFP*, *35Spro:RLK7-Flag 35Spro:prePIP1-GFP*, or *35Spro:RLK7-Flag* were extracted with IP buffer (10-mM Tris–HCl [pH 7.5], 150-mM NaCl, 2-mM EDTA, 1-mM PMSF, and 0.5% [v/v] Nonidet P-40) and incubated with anti-Flag antibody-conjugated agarose (MBL, Aichi, Japan; M185-10). For immunoblot analysis, equal amounts of each sample were separated on a 10% (w/v) SDS–PAGE and transferred to PVDF membranes. Proteins were then probed by immunoblot analysis using anti-Flag (Solarbio, Beijing, China; M1001060) and anti-GFP (Solarbio; M1001030) antibodies.

Determination of RLK7 and MPK3/6 phosphorylation

Phosphorylation of RLK7 was determined as previously described with minor modifications (Chen et al., 2016). Briefly, 10-day-old *35Spro:RLK7-GFP* and *pip3 35Spro:RLK7-GFP* seedlings left untreated or treated with 125-mM NaCl or 1-μM synthetic PIP3 for indicated time period were homogenized in 200-μL protein extracting buffer (50-mM Tris–HCl [pH 8.0], 10-mM $MgCl_2$, 100-mM NaCl, 1-mM DTT, and 1-mM PMSF) containing 1% (v/v) Triton X-100. The samples were subjected to electrophoresis on 10% (w/v) SDS–PAGE gel (with 28% [v/v] glycerol instead of ddH_2O), using sequential voltage steps (70 V/1.5 h, 90 V/1.5 h, up to 120 V for 4 h), and probed by immunoblot analysis using anti-GFP antibody. The ratio between phosphorylated and nonphosphorylated RLK7 (+p/−p) was quantified using Image Lab software (version 2.0.1). For phosphatase treatment, the resulted samples were divided into two aliquots and preheated at 65°C for 15 min to inactivate endogenous phosphatase. rSAP (NEB; M0371S) was then added to one of the two aliquots, and both were incubated at 30°C for 10 min. The reactions were finally stopped by adding 10 μL 5 × loading buffer. Electrophoresis and immunoblot analysis was then performed as described above.

To determine MPK3/6 activation, 10-day-old Col-0, *rlk7-2*, and *pip3* seedlings were left untreated or treated with 125-mM NaCl or 1 μM synthetic PIP3 for indicated periods of time, and the activation of MPK3/6 in Col-0, *rlk7-2* as well as *pip3* seedlings was determined using phospho-p44/42 MAPK (Cell Signaling, Danvers, MA, USA; 9101S) antibodies as previously described (Zhao et al., 2017).

Measurements of chlorophyll fluorescence

Chlorophyll fluorescence was analyzed using a chlorophyll fluorometer (IMAG-MINI PAM-2000) at room temperature. Briefly, 2-week-old soil-grown Col-0 and *rlk7* mutant seedlings were left untreated or treated with 300-mM NaCl for 7 days before being subjected to chlorophyll fluorescence determination. Specifically, seedlings were dark-adapted for 30 min before measurements. Values of F_v/F_m were averaged from equal circles of interested area in leaves. Chlorophyll fluorescence images and chlorophyll fluorescence parameters of the samples were measured synchronously using the Imaging PAM software.

Na^+ content determination using CoroNa Green staining

The Na^+-specific fluorescent dye, CoroNa Green (Invitrogen; C36676), was used to determine Na^+ accumulation in root tips. Four-day-old seedlings grown on MS medium were transferred to fresh liquid medium containing 125-mM NaCl or no NaCl for 12 h. The seedlings were then washed 4 times with distilled water and stained with 20 μM CoroNa Green in the presence of 0.02% (v/v) pluronic acid for 3 h. Fluorescence was visualized under a Leica SP5 confocal microscopy. The mean fluorescence intensity was quantified using ImageJ (version 1.8.0; Schneider et al., 2012). After opening 16-bit image files captured with the confocal laser microscopy, the color threshold was set using the menu Image > Adjust > Color Threshold. The area over the designated threshold was then set automatically with the red demarcation line. The mean fluorescence intensity (mean gray value) was calculated by the menu Analyze > Measure (Ctrl + M). The values were demonstrated as 'Mean' on the pop-up. Nine root tips were analyzed per group for experiments.

Determination of the contents of Na^+ and K^+

Na^+ and K^+ content determination was performed as previously described (Zhou et al., 2012). Two-week-old Col-0, PIP3-OX, or *rlk7* seedlings were treated with 300-mM NaCl for 7 days, and the shoot and root tissues were harvested separately and dried at 80°C for 2 days. The samples were

accurately weighed and treated at 300°C for 1 h and at 575°C for 4 h in a muffle furnace. The resulting ground dry matter was dissolved in 0.1-M HCl. The Na^+ and K^+ contents of the samples were determined with an AAS (Hitachi Z-5000).

Chlorophyll content determination

Entire seedlings or the leaf discs of salt-stressed seedlings grown in liquid MS or on soil were used for the measurements. Chlorophyll was extracted with 80% (v/v) acetone and the absorbance of the extracted solution was measured at 646 and 663 nm. Chlorophyll content was calculated using the following formula: Chl = 17.32 × A646 + 7.18 × A663.

Promoter activity analysis

For GUS staining, a 1,702-bp *prePIP3* genomic DNA fragment upstream of the translational start site (ATG, with A set as position 1) was amplified with primers containing BamHI and NcoI restriction sites and then cloned into the pCAMBIA 1301-GUS vector. Similarly, a 1,672-bp *RLK7* genomic DNA fragment upstream of the ATG was amplified with primers containing EcoRI and NcoI restriction sites and then cloned into the pCAMBIA 1301-GUS vector. The resulting constructs were subsequently transformed into Col-0 and transgenic T_2 lines were used for GUS staining as described (Cheng et al., 2013). The sequences of primers used are listed in Supplemental Table S1.

RT-PCR and RT-qPCR assays

Total RNA was extracted with Trizol reagent (Invitrogen; AM1830) from 10-day-old seedlings grown on MS medium with indicated treatment. Subsequently, total RNA was treated with RNase-free DNase I (Invitrogen; AM2222) to remove genomic DNA. Ten micrograms of RNA was used for reverse transcription with M-MLV reverse transcriptase (Promega, Madison, WI, USA; M1705) according to the manufacturer's instructions. The resulted cDNAs were used for RT-qPCR or PCR analysis to determine the transcription level of *PIP/PIPL* family members as well as *RLK7* using specific primers provided in Supplemental Table S2. *ACTIN 2* was used as an internal control.

Database, sequence alignment, and phylogenetic analysis

The Arabidopsis Genome Initiative, GenBank/EMBL, and Ensembl were used to obtain the information of the *PIP/PIPL* gene family. Predicted AA sequences were aligned by the Clustal W and a phylogenetic tree was constructed by MEGA6 software with the neighbor-joining method (Saitou and Nei, 1987; Tamura et al., 2013).

Statistical analysis

Data are presented as the means ± standard deviation (SD) from three biological replicates if not specified otherwise. For fresh weight measurements, three seedlings or six seedlings per group from one experiment were pooled to determine their total weight as one data point, and three independent experiments made three points ($n = 3$). For root length measurements, the primary root length of nine seedlings per group from three independent experiments was quantified ($n = 9$). For chlorophyll content measurements, six seedlings or six leaf discs from seedlings grown on soil per group from one experiment were pooled to determine chlorophyll contents toward their fresh weight as one data point, and three independent experiments made three points ($n = 3$). For mean fluorescence intensity measurements, nine root tips were analyzed per group from three independent experiments ($n = 9$). For chlorophyll fluorescence measurements, values of F_v/F_m were averaged from six equal circles of interested area in leaves per group from one experiment ($n = 6$). For Na^+ and K^+ content measurements, about 1 g shoots or 0.5 g roots per group from one experiment were pooled for ionic content determination as one data point, and three independent experiments made three points ($n = 3$). For the ratio of +p/−p measurement, the signal intensity quantified from one experiment made one data point, and three independent experiments made three points ($n = 3$). For statistical significance, one-way analysis of variance test was performed, with different lowercase letters indicating a significant difference at $P < 0.05$. Summary of statistical analyses can be found in Supplemental Data Set S1.

Accession numbers

Sequence data from this article can be found in the Arabidopsis Genome Initiative or GenBank/EMBL databases under the following accession numbers: *RLK7* (At1g09970), *prePIP1* (At4g28460), *prePIP2* (At4Gg7290), *prePIP3* (At2g23270), *prePIPL1* (At1g49800), *prePIPL2* (At3g06090), *prePIPL3* (At4g37295), *prePIPL4* (At5g43066), *prePIPL5* (At5g43068), *prePIPL7* (At4g11402), *prePIPL8* (At5g43064), *MPK3* (At3g45640), *MPK6* (At2g43790), *PIP2;1* (At3g53420), and *BIK1* (At2g39660).

Supplemental data

The following materials are available in the online version of this article.

Supplemental Figure S1. Validation of related transgenic plants.

Supplemental Figure S2. Salt sensitivity analyses of transgenic plants overexpressing *PIP/PIPL* members.

Supplemental Figure S3. Determination of the Na^+/K^+ ratio in plants.

Supplemental Figure S4. Overexpression of *prePIP3* enhances plant salt tolerance.

Supplemental Figure S5. Construction of the *pip3* mutant and salt sensitivity analyses.

Supplemental Figure S6. PIP1 is not implicated in plant salt tolerance regulation.

Supplemental Figure S7. Validation of transgenic plants using immunoblot analyses.

Supplemental Figure S8. Validation of *rlk7* mutants and analysis of the subcellular localization of RLK7.

Supplemental Figure S9. RLK7 functions in plant cellular ionic homeostasis regulation.

Supplemental Figure S10. Determination of *prePIP3* and *RLK7* promoter activity.

Supplemental Figure S11. Quantification of the ratio between phosphorylated RLK7 and nonphosphorylated RLK7.

Supplemental Table S1. Primers used for plasmid construction.

Supplemental Table S2. Primers used for RT-qPCR and RT-PCR assays.

Supplemental Table S3. Sequence information of PIP1 and PIP3.

Supplemental File S1. Multiple protein alignment used for the phylogenetic tree shown in Figure 1.

Supplemental File S2. Newick file format of the phylogenetic tree based on Supplemental File S1.

Supplemental Data Set S1. Summary of statistical analyses.

Acknowledgments

We thank Dr Juan Xu from Zhejiang University for kindly providing *mpk3-1* and *mpk6-2* mutants, and Dr Kang Chong from Institute of Biology, CAS for kindly providing the PIP2;1-mCherry-expressing plasmid.

Funding

This work was supported by the National Natural Science Foundation of China (NSFC) (Grants 32170295 and 31870241 to H.Z.; Grant 31970263 to H.L.), the Innovation Spark Fund of Sichuan University (Grant 2019SCUH0011 to H.Z.), the Young Leading Talents Cultivation Project Fund of Sichuan University (Grant 2020-YLTCP-21 to H.Z.), and the Institutional Research Fund of Sichuan University (Grant 2020SCUNL212 to H.L.).

Conflict of interest statement. None declared.

References

Asai T, Tena G, Plotnikova J, Willmann MR, Chiu WL, Gomez-Gomez L, Boller T, Ausubel FM, Sheen J (2002) MAP kinase signalling cascade in Arabidopsis innate immunity. Nature **415**: 977–983

Chang R, Jang CJ, Branco-Price C, Nghiem P, Bailey-Serres J (2012) Transient MPK6 activation in response to oxygen deprivation and reoxygenation is mediated by mitochondria and aids seedling survival in Arabidopsis. Plant Mol Biol **78**: 109–122

Cheeseman J (2016) Food security in the face of salinity, drought, climate change, and population growth. Halophytes for Food Security in Dry Lands, Elsevier, Amsterdam, Netherlands, pp 111–123

Chen J, Yu F, Liu Y, Du C, Li X, Zhu S, Wang X, Lan W, Rodriguez PL, Liu X, et al. (2016) FERONIA interacts with ABI2-type phosphatases to facilitate signaling cross-talk between abscisic acid and RALF peptide in Arabidopsis. Proc Natl Acad Sci USA **113**: E5519–E5527

Chen YL, Fan KT, Hung SC, Chen YR (2020) The role of peptides cleaved from protein precursors in eliciting plant stress reactions. New Phytol **225**: 2267–2282

Cheng MC, Liao PM, Kuo WW, Lin TP (2013) The Arabidopsis ETHYLENE RESPONSE FACTOR1 regulates abiotic stress-responsive gene expression by binding to different cis-acting elements in response to different stress signals. Plant Physiol **162**: 1566–1582

Cristina MS, Petersen M, Mundy J (2010) Mitogen-activated protein kinase signaling in plants. Annu Rev Plant Biol **61**: 621–649

Chien PS, Nam HG, Chen YR (2015) A salt-regulated peptide derived from the CAP superfamily protein negatively regulates salt-stress tolerance in Arabidopsis. J Exp Bot **66**: 5301–5313

Droillard MJ, Boudsocq M, Barbier-Brygoo H, Laurière C (2002) Different protein kinase families are activated by osmotic stresses in *Arabidopsis thaliana* cell suspensions: involvement of the MAP kinases AtMPK3 and AtMPK6. FEBS Lett **527**: 43–50

Evrard A, Kumar M, Lecourieux D, Lucks J, von Koskull-Döring P, Hirt H (2013) Regulation of the heat stress response in Arabidopsis by MPK6-targeted phosphorylation of the heat stress factor HsfA2. Peerj **1**: e59

Feng W, Kita D, Peaucelle A, Cartwright HN, Doan V, Duan Q, Liu MC, Maman J, Steinhorst L, Schmitz-Thom I, et al. (2018) The FERONIA receptor kinase maintains cell-wall integrity during salt stress through Ca^{2+} signaling. Curr Biol **28**: 666–675.e665

Gou X, He K, Yang H, Yuan T, Lin H, Clouse SD, Li J (2010) Genome-wide cloning and sequence analysis of leucine-rich repeat receptor-like protein kinase genes in *Arabidopsis thaliana*. BMC Genomics **11**: 19

Gómez-Gómez L, Boller T (2000) FLS2: an LRR receptor–like kinase involved in the perception of the bacterial elicitor flagellin in Arabidopsis. Mol Cell **5**: 1003–1011

Hohmann U, Lau K, Hothorn M (2017) The structural basis of ligand perception and signal activation by receptor kinases. Ann Rev Plant Biol **68**: 109–137

Hou S, Wang X, Chen D, Yang X, Wang M, Turra D, Di Pietro A, Zhang W (2014) The secreted peptide PIP1 amplifies immunity through receptor-like kinase 7. PLoS Pathog **10**: e1004331

Jinn TL, Stone JM, Walker JC (2000) HAESA, an Arabidopsis leucine-rich repeat receptor kinase, controls floral organ abscission. Genes Dev **14**: 108–117

Kondo T, Sawa S, Kinoshita A, Mizuno S, Kakimoto T, Fukuda H, Sakagami Y (2006) A plant peptide encoded by CLV3 identified by in situ MALDI-TOF MS analysis. Science **313**: 845–848

Lease KA, Walker JC (2010) Bioinformatic identification of plant peptides. Peptidomics, Springer, Berlin, Germany, pp 375–383

Li CH, Wang G, Zhao JL, Zhang LQ, Ai LF, Han YF, Sun DY, Zhang SW, Sun Y (2014) The receptor-like kinase SIT1 mediates salt sensitivity by sctivating MAPK3/6 and regulating ethylene homeostasis in rice. Plant Cell **26**: 2538–2553

Li J, Zhou H, Zhang Y, Li Z, Yang Y, Guo Y (2020) The GSK3-like kinase BIN2 is a molecular switch between the salt stress response and growth recovery in *Arabidopsis thaliana*. Dev Cell **55**: 367–380

Li J, Chory J (1997) A putative leucine-rich repeat receptor kinase involved in brassinosteroid signal transduction. Cell **90**: 929–938

Ma Y, Dai X, Xu Y, Luo W, Zheng X, Zeng D, Pan Y, Lin X, Liu H, Zhang D, et al. (2015) COLD1 confers chilling tolerance in rice. Cell **160**: 1209–1221

Macho AP, Lozano-Durán R, Zipfel C (2015) Importance of tyrosine phosphorylation in receptor kinase complexes. Trends Plant Sci **20**: 269–272

Matsubayashi Y, Yang H, Sakagami Y (2001) Peptide signals and their receptors in higher plants. Trends Plant Sci **6**: 573–577

Matsubayashi Y (2011) Post-translational modifications in secreted peptide hormones in plants. Plant Cell Physiol **52**: 5–13

Matsubayashi Y (2014) Posttranslationally modified small-peptide signals in plants. Annu Rev Plant Biol **65**: 385–413

Matsubayashi Y, Sakagami Y (2006) Peptide hormones in plants. Annu Rev Plant Biol **57**: 649–674

Meng X, Wang H, He Y, Liu Y, Walker JC, Torii KU, Zhang S (2012) A MAPK cascade downstream of ERECTA receptor-like protein kinase regulates Arabidopsis inflorescence architecture by promoting localized cell proliferation. Plant Cell **24**: 4948–4960

Mishra NS, Tuteja R, Tuteja N (2006) Signaling through MAP kinase networks in plants. Arch Biochem Biophys **452**: 55–68

Moon H, Lee B, Choi G, Shin D, Prasad DT, Lee O, Kwak SS, Kim DH, Nam J, Bahk J, et al. (2003) NDP kinase 2 interacts with two oxidative stress-activated MAPKs to regulate cellular redox state and enhances multiple stress tolerance in transgenic plants. Proc Natl Acad Sci USA **100**: 358–363

Munns R, Tester M (2008) Mechanisms of salinity tolerance. Annu Rev Plant Biol **59**: 651–681

Murphy E, Smith S, De Smet I (2012) Small signaling peptides in Arabidopsis development: how cells communicate over a short distance. Plant Cell **24**: 3198–3217

Nakaminami K, Okamoto M, Higuchi-Takeuchi M, Yoshizumi T, Yamaguchi Y, Fukao Y, Shimizu M, Ohashi C, Tanaka M, Matsui M, et al. (2018) AtPep3 is a hormone-like peptide that plays a role in the salinity stress tolerance of plants. Proc Natl Acad Sci USA **115**: 5810–5815

Oh DH, Lee SY, Bressan RA, Yun DJ, Bohnert HJ (2010) Intracellular consequences of SOS1 deficiency during salt stress. J Exp Bot **61**: 1205–1213

Osakabe Y, Yamaguchi-Shinozaki K, Shinozaki K, Tran LSP (2013) Sensing the environment: key roles of membrane-localized kinases in plant perception and response to abiotic stress. J Exp Bot **64**: 445–458

Pitorre D, Llauro C, Jobet E, Guilleminot J, Brizard JP, Delseny M, Lasserre E (2010) RLK7, a leucine-rich repeat receptor-like kinase, is required for proper germination speed and tolerance to oxidative stress in *Arabidopsis thaliana*. Planta **232**: 1339–1353

Saitou N, Nei M (1987) The neighbor-joining method: a new method for reconstructing phylogenetic trees. Mol Biol Evol **4**: 406–425

Schneider CA, Rasband WS, Eliceiri KW (2012) NIH Image to ImageJ: 25 years of image analysis. Nat Methods **9**: 671–675

Shiu SH, Karlowski WM, Pan R, Tzeng YH, Mayer KF, Li WH (2004) Comparative analysis of the receptor-like kinase family in Arabidopsis and rice. Plant Cell **16**: 1220–1234

Shinohara H, Moriyama Y, Ohyama K, Matsubayashi Y (2012) Biochemical mapping of a ligand-binding domain within Arabidopsis BAM1 reveals diversified ligand recognition mechanisms of plant LRR-RKs. Plant J **70**: 845–854

Smékalová V, Doskočilová A, Komis G, Šamaj J (2014) Crosstalk between secondary messengers, hormones and MAPK modules during abiotic stress signalling in plants. Biotechnol Adv **32**: 2–11

Takahashi F, Mizoguchi T, Yoshida R, Ichimura K, Shinozaki K (2011) Calmodulin-dependent activation of MAP kinase for ROS homeostasis in Arabidopsis. Mol Cell **41**: 649–660

Takahashi F, Suzuki T, Osakabe Y, Betsuyaku S, Kondo Y, Dohmae N, Fukuda H, Yamaguchi-Shinozaki K, Shinozaki K (2018) A small peptide modulates stomatal control via abscisic acid in long-distance signalling. Nature **556**: 235–238

Takahashi F, Hanada K, Kondo T, Shinozaki K (2019) Hormone-like peptides and small coding genes in plant stress signaling and development. Curr Opin Plant Biol **51**: 88–95

Tamura K, Stecher G, Peterson D, Filipski A, Kumar S (2013) MEGA6: molecular evolutionary genetics analysis version 6.0. Mol Biol Evol **30**: 2725–2729

Tian M, Lou L, Liu L, Yu F, Zhao Q, Zhang H, Wu Y, Tang S, Xia R, Zhu B, Serino G, Xie Q (2015) The RING finger E3 ligase STRF1 is involved in membrane trafficking and modulates salt-stress response in *Arabidopsis thaliana*. Plant J **82**: 81–92

Torii KU (2004) Leucine-rich repeat receptor kinases in plants: structure, function, and signal transduction pathways. Int Rev Cytol **234**: 1–46

Toyokura K, Goh T, Shinohara H, Shinoda A, Kondo Y, Okamoto Y, Uehara T, Fujimoto K, Okushima Y, Ikeyama Y, et al. (2019) Lateral inhibition by a peptide hormone-receptor cascade during Arabidopsis lateral root founder cell formation. Dev Cell **48**: 64–75

Van Zelm E, Zhang Y, Testerink C (2020) Salt tolerance mechanisms of plants. Annu Rev Plant Biol **71:** 403–433

Vie AK, Najafi J, Liu B, Winge P, Butenko MA, Hornslien KS, Kumpf R, Aalen RB, Bones AM, Bremb T (2015) The IDA/IDA-LIKE and PIP/PIP-LIKE gene families in Arabidopsis: phylogenetic relationship, expression patterns, and transcriptional effect of the PIPL3 peptide. J Exp Bot **66**: 5351–5365

Wang ZP, Xing HL, Dong L, Zhang HY, Han CY, Wang XC, Chen QJ (2015) Egg cell-specific promoter-controlled CRISPR/Cas9 efficiently generates homozygous mutants for multiple target genes in Arabidopsis in a single generation. Genome Biol **16**: 144

Yang Y, Guo Y (2018) Unraveling salt stress signaling in plants. J Integr Plant Biol **60**: 796–804

Yu L, Nie J, Cao C, Jin Y, Yan M, Wang F, Liu J, Xiao Y, Liang Y, Zhang W (2010) Phosphatidic acid mediates salt stress response by regulation of MPK6 in *Arabidopsis thaliana*. New Phytol **188**: 762–773

Zhao C, Wang P, Si T, Hsu CC, Wang L, Zayed O, Yu Z, Zhu Y, Dong J, Tao WA, et al. (2017) MAP kinase cascades regulate the cold response by modulating ICE1 protein stability. Dev Cell **43**: 618–629 e615

Zhao C, Zayed O, Yu Z, Jiang W, Zhu P, Hsu CC, Zhang L, Tao WA, Lozano-Durán R, Zhu JK (2018) Leucine-rich repeat extensin proteins regulate plant salt tolerance in Arabidopsis. Proc Natl Acad Sci USA **115**: 13123–13128

Zhou H, Zhao J, Yang Y, Chen C, Liu Y, Jin X, Chen L, Li X, Deng XW, Schumaker KS, et al. (2012) Ubiquitin-specific protease16 modulates salt tolerance in Arabidopsis by regulating Na^+/H^+ antiport activity and serine hydroxymethyltransferase stability. Plant Cell **24**: 5106–5122

Zhou H, Lin H, Chen S, Becker K, Yang Y, Zhao J, Kudla J, Schumaker KF, Guo Y (2014) Inhibition of the Arabidopsis salt overly sensitive pathway by 14-3-3 proteins. Plant Cell **26**: 1166–1182

Zhu JK (2016) Abiotic stress signaling and responses in plants. Cell **167**: 313–324